The Magazine for Nanoscience and Technology

VOL 29. 2025

NANOscientific

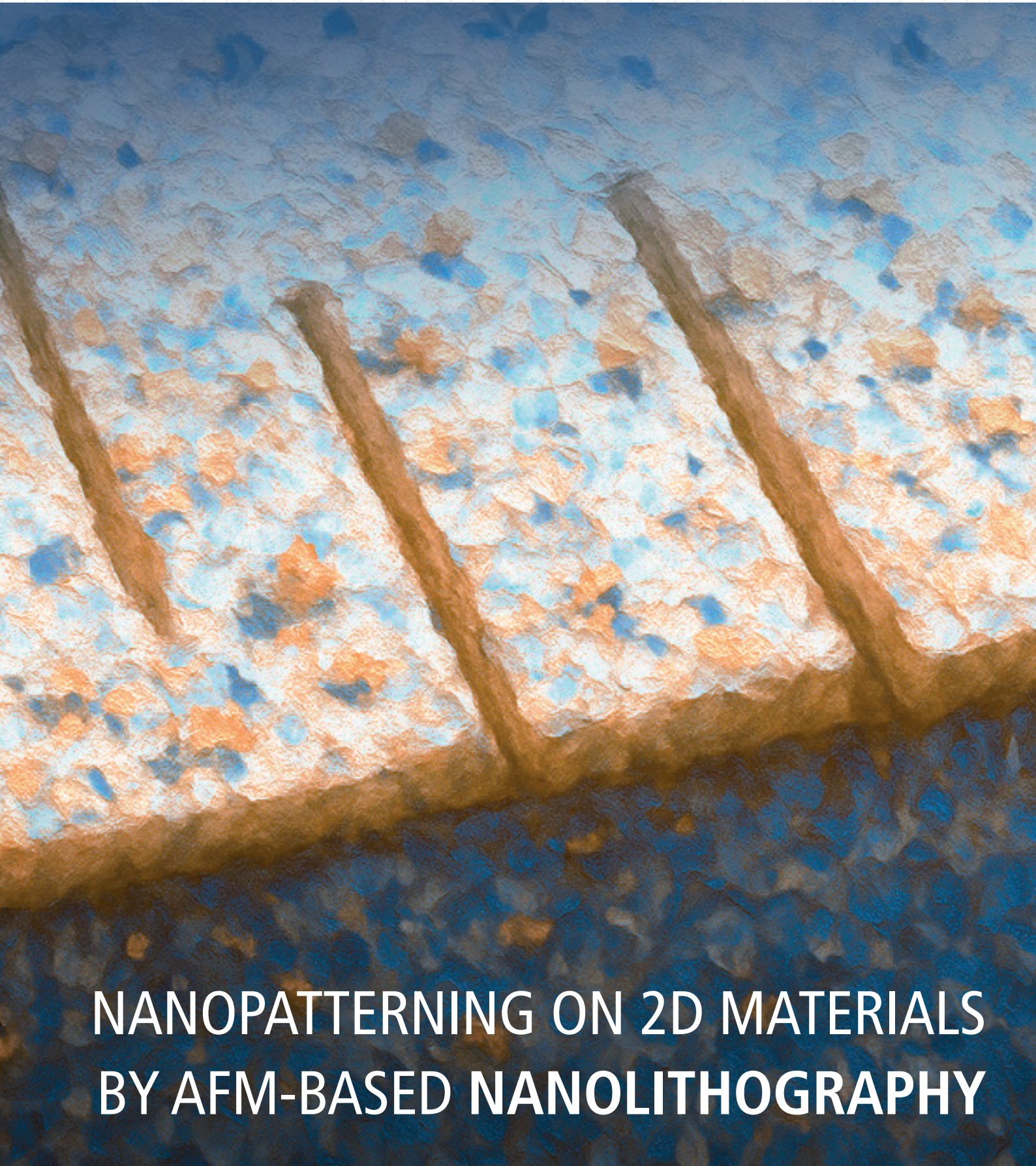

NANOPATTERNING ON 2D MATERIALS BY AFM-BASED **NANOLITHOGRAPHY**

NANOPATTERNING ON 2D MATERIALS BY AFM-BASED NANOLITHOGRAPHY

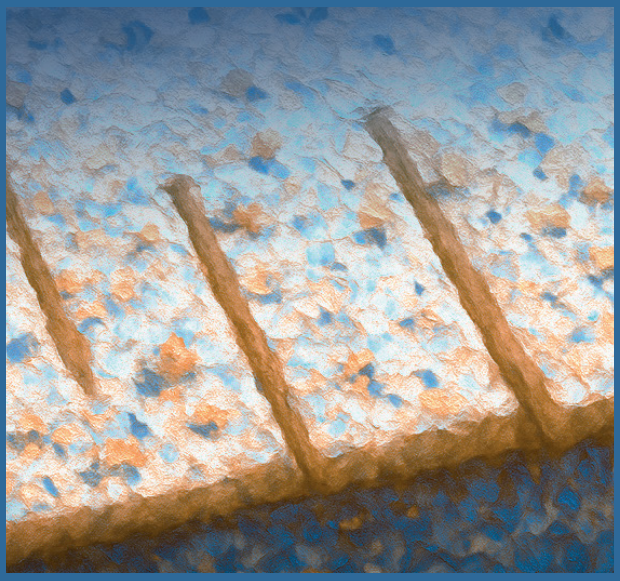

This issue's cover features an artistically rendered image inspired by cutting direction analysis in AFM-based nanolithography on graphene. The visual showcases how the approach speed of the AFM tip—when carefully slowed—eliminates directional dependency, enabling clean, uniform cuts in any orientation. The design retains the intricate nanoscale patterns from the original figure while enhancing contrast and composition: the upper region has been darkened from its original golden hue to visually unify the layered structure and avoid misinterpretation of where the cutting occurs. A subtle zoom and shift remove the upper-left corner gap created by the image's original 3D tilt, which had been angled from the lower right to accentuate depth. This reimagined visualization captures the essence of next-generation nanofabrication—where control, consistency, and creativity converge at the atomic scale.

About this issue

In this 29th volume of NanoScientific Magazine, we highlight key advances from the recent NanoScientific Symposium Series across the Americas, Europe, and Asia. This issue brings together innovative research in optical, electrical, and force-based microscopy. From SNOM and ellipsometry studies of polaritons and excitons in the Americas, to breakthroughs in electrical SPM, PFM, and MFM in Europe, and high-throughput 3D-AFM and semiconductor applications in Asia, each article showcases the expanding role of nanoscale metrology in science and industry. An application note on AFM-based nanolithography for 2D materials rounds out this global perspective on the future of nanoscience.

INDEX

NANO scientific

- **Keibock Lee**, Editor-in-Chief (keibock@nanoscientific.org)
- **SangMin Yi**, Managing Editor
- **Peter Park**, Editor and Point of Contact (peter.park@parksystems.com)
- **Cathy Lee**, Technical Editor
- **Ester Cho**, Art Director

Publisher and Corporate officers

- **Sang-il Park**, Chief Executive Officer
- **Karen Cho**, Senior EVP of Operations Management
- **Ryan Yoo**, Senior EVP of Business Development
- **Sang-Joon Cho**, EVP of Research Equipment Business Unit
- **Richard Lee**, EVP of Industrial Equipment Business Unit

NanoScientific is published both in print and online to showcase advancements in the field of nanoscience and technology across a wide range of multidisciplinary areas of research. The publication is offered free to anyone who works or have interest in the field of nanotechnology, nanoscience, microscopy and other related fields of study and manufacturing.
We enjoy hearing from you, our readers.
Please send your research or story ideas to peter.park@parksystems.com.
To view all of our articles, please visit our web site at nanoscientific.org.

NANO
scientific

NANOscientific Symposium 2025

Explore the Future of Nanoscience

The 2025 NANOscientific Symposium will bring together leading experts worldwide to share the latest advancements in nanoscience and technology. This year, it expands beyond scanning probe microscopy to cover a broader range of nanotechnology applications and innovations.

The agenda includes keynote presentations from respected industry and academic leaders, interactive sessions, and enhanced virtual networking. Attendees will gain valuable insights, access resources to advance their research, and connect with peers to foster meaningful collaborations in this evolving field.

Join us and stay at the forefront of nanoscience.

nanoscientific.org/nss2025

NSS Korea
Aug 28 | KANC, Suwon

NSF Europe
Sep 17 - 19 | Orsay, France

NSS India
Oct 15 - 16 | IISc, Bangalore

NSS Japan
Oct 24 | University of Tokyo, Tokyo

NSS Americas: 40 Years of AFM
In Memory of Prof. Calvin Quate
Dec 02 - 03 | Stanford University, USA

Sponsored by

Park SYSTEMS

NANOTECHNOLOGY WORLD

NANOSTRUCTURED INORGANIC SEMICONDUCTORS FOR ADVANCED OPTOELECTRONICS: THE ROLE OF ATOMIC FORCE MICROSCOPY

Assistant Professor Munho Kim, Nanyang Technological University, Singapore
Adapted from Presentation, Edited by NanoScientific

In the fast-moving realm of advanced optoelectronic devices, control of material properties at the nanoscale is a decisive factor for performance and innovation. Assistant Professor Munho Kim of Nanyang Technological University, Singapore, is pushing these boundaries through the development of unconventional semiconductor structures and device concepts. His research focuses on inorganic semiconductor nanomembranes and nanostructured architectures, with Atomic Force Microscopy (AFM) serving as a critical tool in characterizing and refining these nanoscale innovations.

This feature explores the two key areas of his research: ultra-thin crystalline semiconductor nanomembranes and high-aspect-ratio nanostructures fabricated via metal-assisted chemical etching (MACE). Both highlight AFM's essential role in precision engineering, device optimization, and surface quality validation.

Quasi-2D Semiconductor Nanomembranes

At the core of Prof. Kim's work lies the creation of quasi-two-dimensional semiconductor nanomembranes—ultrathin, flexible crystalline layers of materials like silicon, germanium, and gallium nitride. These membranes, with thicknesses ranging from hundreds down to just 10 nanometers, retain exceptional electrical and optoelectronic properties, including high carrier mobility and minimal defect density.

Such membranes can be transferred to a variety of substrates—rigid or flexible—by exploiting oxide sacrificial layers in silicon-on-insulator (SOI) or germanium-on-insulator (GeOI) wafers. Selective etching in hydrofluoric acid releases the top layer, which is then transfer-printed onto the target substrate. This technique combines the mechanical flexibility of a thin film with the high material quality of bulk crystals, paving the way for applications in wearable sensors, flexible electronics, and integrated optoelectronic systems.

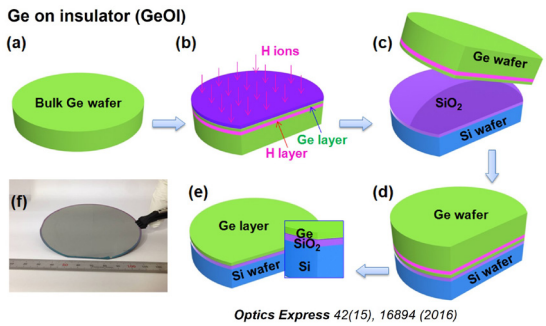

Fig. 1. *Schematic fabrication process for 4-inch Ge on insulator substrates using the wafer bonding and hydrogen ion implantation*

Enhancing Light Absorption in Ultra-Thin Layers

Reducing the thickness of semiconductors usually compromises light absorption. Prof. Kim's lab has addressed this by using optical cavity effects to recycle light within the structure. By placing ultrathin germanium layers—7 to 25 nm—on reflective metals such as silver or gold, light undergoes multiple internal reflections, boosting absorption up to 80% despite the reduced material volume.

However, high absorption alone is not enough; crystallinity matters. Conventional deposition at these thicknesses often yields amorphous or polycrystalline films, degrading device performance. To overcome this, the team fabricates single-crystalline nanomembranes via smart-cut processes and wafer bonding, followed by chemical mechanical polishing (CMP). AFM measurements confirm post-polishing surface roughness as low as 0.6 nm, a key metric for reducing defect densities and improving device efficiency.

Device Applications: Phototransistors with Nanocavity Designs

Using these high-quality membranes, the group has demonstrated devices such as phototransistors built on aluminum oxide/silver stacks that function as optical nanocavities. The devices exhibit strong wavelength-specific response and high normalized photo-to-dark current ratios (NPDR). Notably, membrane thickness controls the spectral absorption peak, allowing device tuning for specific optical ranges.

At around 20 nm thickness, the depletion width exceeds the active layer, lowering dark current and enhancing detection sensitivity. AFM's precision measurements of membrane step heights and surface topography are crucial in correlating physical structure to device performance.

Nanostructures via Metal-Assisted Chemical Etching (MACE)

In parallel, Prof. Kim's group develops high-aspect-ratio semiconductor nanostructures through MACE. This scalable technique uses a thin metal catalyst layer, typically gold or platinum, deposited on semiconductors like silicon, silicon carbide, or gallium oxide. Immersion in an etchant solution triggers redox reactions at the metal interface, generating holes that oxidize the semiconductor beneath. The oxidized regions are then etched away, leaving pillars, wires, or porous structures with nanoscale precision.

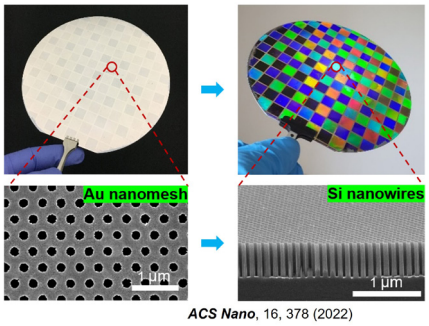

Fig. 2. *Transfer-printing of Au meshes on 6-inch Si substrate and MACE for wafer-scale uniform Si nanowires*

Control of carrier generation and mass transport determines etch geometry and quality. Variants such as forward MACE, inverse MACE, self-anchored MACE, and photo-enhanced MACE (for wide bandgap semiconductors) broaden the design possibilities. In materials like gallium oxide, photo-enhanced MACE uses UV illumination to generate sufficient carriers for efficient etching.

AFM as a Critical Tool in MACE Optimization

AFM's role in MACE-based nanostructuring is indispensable. It provides:

- **Topography Mapping:** High-resolution imaging of etched surfaces to verify structure dimensions.
- **Surface Roughness Analysis:** Ensuring smoothness for reduced defect sites in subsequent device fabrication.
- **Depth and Height Profiling:** Measuring aspect ratios of nanostructures with sub-nanometer accuracy.

For example, AFM imaging of MACE-etched silicon carbide reveals nanohole arrays over 100 nm deep, with etched ridge features corresponding precisely to SEM observations. Similar measurements in gallium oxide quantify nanoridge heights of ~160 nm. These insights enable fine-tuning of etching parameters to achieve desired structure geometries and surface finishes.

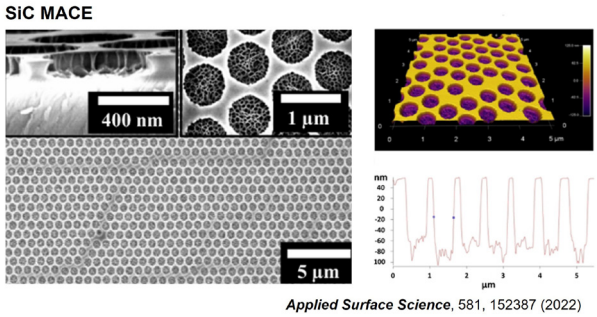

Fig. 3. *MACE for 4H-SiC nanohole array (SEM and AFM images)*

Implications for Advanced Optoelectronics

The nanomembranes and nanostructures emerging from Prof. Kim's lab have wide-ranging implications:

- **Flexible and Wearable Electronics:** Transferrable nanomembranes enable integration onto diverse substrates.
- **High-Sensitivity Photodetectors:** Optical nanocavities amplify light absorption in ultrathin active layers.
- **Power Electronics:** Wide bandgap semiconductor nanostructures promise improved thermal and voltage handling.
- **Next-Generation Imaging:** Tunable devices span ultraviolet to infrared detection ranges.

AFM remains at the center of these advances, bridging material synthesis and device integration by ensuring nanoscale precision in every step.

Conclusion

Prof. Kim's work exemplifies the synergy between advanced materials engineering and state-of-the-art characterization. By pairing innovative semiconductor architectures with AFM's unmatched resolution and surface analysis capabilities, his team is advancing the frontier of optoelectronic device design. Future directions include expanding the materials palette to carbonitrides and oxide semiconductors, refining MACE selectivity, and integrating nanostructures into full device platforms.

The research underscores a clear lesson for the field: at the nanoscale, precision is everything—and AFM remains one of the most powerful tools to achieve it.

Acknowledgments

Prof. Kim acknowledges the contributions of his research group and support from Nanyang Technological University, A*STAR, and the Ministry of Education, Singapore.

About Prof. Munho Kim

Dr. Munho Kim is an Assistant Professor in the School of Electrical and Electronic Engineering at Nanyang Technological University (NTU), Singapore. He received his BS and MS degrees from POSTECH and KAIST, and his PhD in Electrical and Computer Engineering from the University of Wisconsin–Madison in 2016. He gained industry experience at Samsung Semiconductor and completed postdoctoral research at the University of Illinois Urbana-Champaign. His work focuses on wide bandgap nanomembranes, flexible electronics, silicon/germanium optoelectronics, and advanced fabrication techniques for next-generation devices.

Prof. Kim (4th from left) and his research group

SPOTTING MOLECULAR EXCITONS: PROBING ORGANIC CRYSTAL TEXTURES WITH IMAGING MUELLER MATRIX ELLIPSOMETRY

Dr. Manuela Schiek, Center for Surface and Nanoanalytics, Johannes Kepler University Linz, Austria; Optical Nanometrology, National Metrology Institute, Braunschweig, Germany. Adapted from Presentation, Edited by NanoScientific

Introduction: Turning Light into a Crystal Map

At the 2024 NanoScientific Forum Europe, Dr. Manuela Schiek introduced the audience to the power of Imaging Mueller Matrix Ellipsometry (IMME) for revealing the hidden optical and excitonic properties of complex molecular crystals. Her work focuses on organic semiconductor systems—materials whose optical response is driven by molecular packing and excitonic interactions—demonstrating how IMME can extract complete dielectric tensors and reveal subtle excitonic transitions beyond the reach of standard optical microscopy.

In her talk, Dr. Schiek focused on a noncommercial organic semiconductor known for its intense light–matter interactions. By carefully controlling its crystalline polymorphs through spin-coating and thermal annealing, and by combining polarized microscopy with Mueller matrix ellipsometry, she and her collaborators have mapped Davydov-split excitonic transitions, quantified dielectric tensors for orthorhombic crystals and identified dark states. Her results show how advanced ellipsometric imaging can link molecular orientation, crystal symmetry, and optical anisotropy at a quantitative level.

The Material System: A Platform for Excitonic Coupling

The organic semiconductor at the center of this work—nicknamed "SQIB"—features a donor–acceptor–donor molecular backbone with side chains that dictate the molecular packing. Although the side chains do not directly participate in light absorption, their steric effects steer the crystal structure, aligning transition dipole moments along the molecular backbone.

When crystallized into rotational domains (platelets) through spin-coating and thermal annealing, the material forms a distinct polymorph. The orthorhombic form—common at elevated annealing temperatures—consists of four molecules per primitive unit cell, preferentially oriented with their (110) plane parallel to the substrate. The molecular arrangement creates strong excitonic coupling between adjacent molecules, resulting in multiple Davydov-split excitonic transitions: two upper and two lower components, one being a dark state, with the polarization directions of the remaining three aligned to crystal axes.

This excitonic structure is more than an optical curiosity—it encodes information about molecular packing, crystal symmetry, and intermolecular interactions. Determining the polarization and energies of these transitions, and correlating them to the underlying crystal lattice, is the core challenge that Mueller matrix ellipsometry addresses.

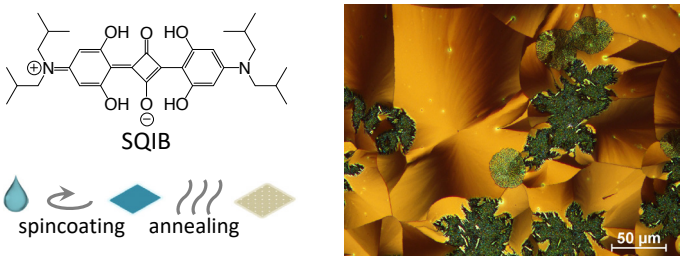

Fig. 1. *The structural formula of SQIB and the sample preparation procedure are sketched on the left. On the right an optical microscope image between crossed polarizers of a SQIB thin film is shown. The golden-brown areas are orthorhombic platelets, while the greenish areas consist of the monoclinic polymorph.*

From Polarized Microscopy to Imaging Mueller Matrix Ellipsometry

Initial characterization begins with polarized optical microscopy, where rotating a linear polarizer across a crystalline platelet reveals characteristic color and intensity changes. These variations directly reflect the polarization of optical transitions. By collecting spectra as a function of polarizer angle, the two main Davydov components can be resolved. Rotating by 90° shifts intensity between the upper and lower components, a signature of orthogonal polarization states.

However, polarized microscopy alone captures only the projected polarization in the sample plane. For a full picture—including out-of-plane components—one must recover the complete dielectric tensor. This requires ellipsometry.

Imaging Mueller Matrix Ellipsometry extends classical ellipsometry by capturing either the full 4×4 or the partial 3×4 Mueller matrix for each pixel of the image. In Dr. Schiek's work, the latter was done using a Nanofilm EP4 system equipped with a single rotating compensator on the incident side and high-magnification objectives providing ~2 µm spatial resolution. Measurements in both reflection and transmission geometries at multiple incidence and azimuthal angles are combined to reconstruct the dielectric tensor for multiple rotational platelet domains.

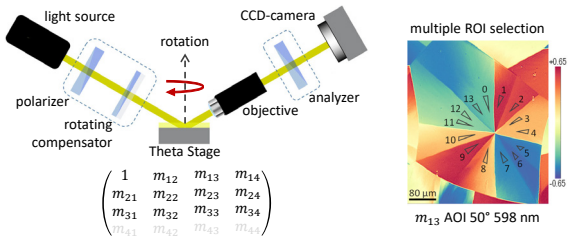

Fig. 2. *On the left is a sketch of the EP4 imaging ellipsometer and a partial Mueller matrix (last row missing). On the right is the m13 element of a platelet structure consisting of several subdomains, for which several regions of interest (ROIs) must be selected for data fitting. The angle of incidence (AOI) for this reflection measurement was 50° and the selected wavelength for imaging was 598 nm.*

Extracting the Dielectric Tensor

The orthorhombic platelet presents an ideal test case: its crystal axes are orthogonal, and the dielectric tensor is diagonal in the crystallographic frame.

Using a combination of fixed-wavelength Mueller matrix maps and azimuthal rotation ("theta scans") at multiple incidence angles, Dr. Schiek's team determines the in-plane crystal orientation, particularly the c-axis direction. Once the orientation is fixed, full spectroscopic ellipsometry can be performed.

The fitting procedure—developed in-house—uses a phenomenological oscillator model constrained by Kramers–Kronig relations to determine the complex dielectric tensor components εa(ω), εb(ω), and εc(ω) in spectral resolution. The results reveal:

- **Multiple Davydov-split excitonic resonances** corresponding to the four molecules in the orthorhombic unit cell.
- **A dark excitonic state**—predicted by group theory but invisible to linear optical spectroscopy—whose presence is inferred from the tensor structure and excitonic polarization analysis.
- **Negative real permittivity** in spectral ranges close to the excitonic resonances, indicating strong intermolecular coupling, which gives rise to the metallic luster of the platelets.

There are three visible Davydov resonances, whereby in the projected view normal to the (110) surface—as is usual in conventional microscopy/spectroscopy— the two lower Davydov components overlap due to their close spectral positions and similar polarization orientations. These tensor measurements directly link the measured optical anisotropy to the molecular packing geometry—something impossible to extract from conventional microscopy.

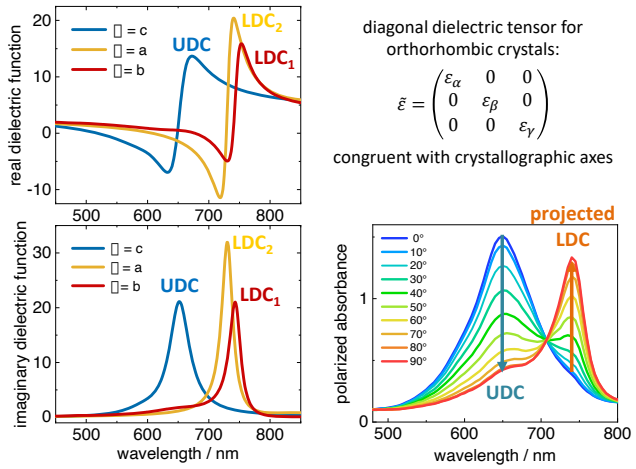

Fig. 3. *The real (upper) and imaginary (lower) parts of the dielectric tensor for orthorhombic SQIB plates are shown on the left. UDC = Upper Davydov Component along crystallographic c-axis. LDC = Lower Davydov Component along the a-axis (LDC_2) and the b-axis (LDC_1). The polarized absorbance spectra on the bottom right for azimuthal rotation angles from 0° to 90° were measured under normal incidence. At 0° UDC is at its maximum while at 90° the projected LDC is at its maximum. The projected LDC is the superposition of LDC_1 and LDC_2.*

The Role of Crystal Symmetry and Polymorphism

An intriguing feature of the SQIB material is its polymorphism. At excessive annealing temperatures, the orthorhombic platelets partially transform to a greenish monoclinic phase, which is thermodynamically more stable despite its lower symmetry.

The monoclinic polymorph has only two molecules per primitive unit cell. Consequently, its Davydov splitting is simpler: just two components (upper and lower), without the dark state present in the orthorhombic form. However, the monoclinic system's oblique lattice means that the polarization of these components is no longer aligned with principal crystal axes. Only one Davydov component lies along the monoclinic b-axis (the principal axis), while the upper component is rotated by an angle other than 90° in the projection.

Using the EP4 system in transmission intensity mode and user-defined measurement routines via the Python interface, Dr. Schiek's group confirms the predicted polarization angles experimentally, with measured orientations matching the calculated non-orthogonal rotational offset for the other Davydov component.

Beyond Orthorhombic: The Challenge of Complex Tensors

For the orthorhombic crystal, the dielectric tensor aligns neatly with crystallographic axes, simplifying analysis. The monoclinic system is more challenging: its tensor components—except for one—are rotated relative to the crystal frame, and this rotation can also depend on the spectral range. In triclinic systems, no tensor component is aligned with the crystal lattice but all tensor components may be coupled.

Schiek notes that extracting the full tensor for monoclinic or triclinic crystals remains an open challenge for the next stage of this research. Developing robust analysis methods for such systems will be crucial to extending Mueller matrix ellipsometry to a wider class of complex organic materials.

Why This Matters: Linking Molecular Design to Optical Function

This work is more than an exercise in ellipsometry—it points to a powerful feedback loop for material design. Organic semiconductors are increasingly used in light-harvesting, sensing, and optoelectronic devices, where excitonic structure determines performance.

By quantitatively linking molecular packing, excitonic splitting, and dielectric anisotropy, Mueller matrix ellipsometry offers a tool to:

- **Characterize new materials** without requiring single-crystal growth or destructive sectioning.
- **Identify polymorphs** and phase transitions through their optical signatures.
- **Support theoretical modeling** such as prediction of dark states by providing experimentally validated tensor data.

Moreover, determining dielectric tensors and exciton transitions is not limited to organic materials but can also be applied to inorganic semiconductors and low-dimensional patterned materials.

Conclusion: Quant. Optical Probe for Complex Mol. Systems

Dr. Schiek's work demonstrates that Imaging Mueller Matrix Ellipsometry can go beyond traditional optical microscopy, delivering quantitative dielectric tensors and revealing excitonic structures in complex organic crystals.

For the orthorhombic polymorph of SQIB, the technique resolves multiple Davydov-split excitons, including a dark state. For the monoclinic form, it confirms the polarization geometry of upper and lower excitonic components. These results not only expand our understanding of excitonic coupling in organic crystals but also point the way toward broader application of IMME in nanomaterials research.

As Dr. Schiek concluded, "Imaging ellipsometry is really cool—you can do something quantitative with it. You can get tensors." In her work, that enthusiasm is backed by rigorous data and careful interpretation, showing how a sophisticated optical technique can turn molecular-scale order into measurable, meaningful parameters.

About Dr. Manuela Schiek

Dr. Manuela Schiek is a Senior Researcher and Lecturer at the Center for Surface and Nano Analytics (ZONA) at the Johannes Kepler University Linz, Austria, and also works in the Optical Nanometrology group at the National Metrology Institute (PTB) in Brunswick, Germany. Her research focuses on (chiral) molecular excitonics, functional organic thin films, and solid–liquid interfaces, with emphasis on polarization-resolved microscopy and spectroscopy. She is particularly interested in ellipsometry in various forms.

Dr. Manuela Schiek (center) with key-publication collaborators Dr. Frank Balzer (left) and Dr. Matthias Duwe (right).

For more information visit : https://orcid.org/0000-0002-0108-2998.

References

1. S. Funke, M. Duwe, F. Balzer, P. H. Thiesen, K. Hingerl, M. Schiek. Determining the Dielectric tensor of Micro-Textured Organic Thin Films by Imaging Mueller Matrix Ellipsometry. J. Phys. Chem. Lett. 12 (2021) 3053-3058. DOI: 10.1021/acs.jpclett.1c00317
2. F. Balzer, T. Breuer, G. Witte, M. Schiek. Template and Temperature-Controlled Polymorph Formation in Squaraine Thin Films. Langmuir 38 (2022) 9266-9277. DOI: 10.1021/acs.langmuir.2c01023
3. D. Giavazzi, R. Schwarzl, M. Koch, M. Schiek, A. Painelli, F. C. Spano. Modeling the Electronic Coupling in Squaraine Thin Films: The Unusual Case of Three Davydov Components. Submitted 2025.

UNLOCKING ADVANCED MATERIAL INSIGHTS WITH IMAGING SPECTROSCOPIC ELLIPSOMETRY

Dr. Mangesh Diware, Park Systems Inc.
Adapted from Presentation, Edited by NanoScientific

Introduction: A New Dimension in Ellipsometry

At the 2024 NanoScientific Symposium, Dr. Mangesh Diware took the audience on a journey through one of the most powerful—and evolving—optical metrology techniques in nanoscience: Imaging Spectroscopic Ellipsometry (ISE). Building on the robust foundations of traditional ellipsometry, ISE integrates high-resolution imaging to evaluate not only thickness and refractive index, but also spatially resolved optical property variations at the micron scale.

Ellipsometry has been a cornerstone in materials science for decades, delivering non-contact, non-destructive characterization of thin films and layered structures. But the challenge has always been lateral resolution, limited by focusing optics. Conventional ellipsometry averages data over tens of microns. ISE changes that—fusing the vertical precision of ellipsometry (down to 0.1 nm) with lateral resolution of approximately 1 µm.

As Dr. Diware described, "The integration of imaging opens entirely new possibilities—seeing not just the average behavior, but the local variations that matter in devices and advanced material science."

Ellipsometry: From the Dark Ages to Imaging Era

The origins of ellipsometry stretch back to the foundational work of Robert Hooke and James Clerk Maxwell. The technique's modern development can be viewed in three stages [1]:

- Dark ages – Before digital electronics, measurements relied on nulling methods, manually adjusting optics until no light was detected. Analysis was slow and highly operator dependent.
- Modern age – The 1970s brought photometric designs and the first computer-controlled systems (notably by Aspens and Sudana), allowing automated data collection.
- Postmodern era – The introduction of photodiode arrays and spectroscopic scanning enabled fast, multi-wavelength acquisition. A 2013 innovation—the three-polarizer configuration—eliminated the wavelength dependence of older compensators.

These advances established ellipsometry as a high-precision optical tool. However, as device geometries shrank and structures grew more complex, the need for lateral resolution became increasingly critical, setting the stage for ISE.

The Physics Behind Ellipsometry: Why Phase Matters

Ellipsometry works by measuring how the polarization of light changes after interaction with the sample surface. Specifically, it tracks the change in amplitude ratio (Ψ) and phase (Δ) between two orthogonal components of the electric field (parallel and perpendicular to the plane of incidence).

Phase sensitivity is key. Even a 0.01° shift in phase can correspond to changes in thickness on the femtometer scale. In practice, ellipsometry can detect sub-nanometer thickness differences.

Use of different spectral ranges helps to probe different physical properties:

- UV–Visible – Band structure, band gap energies, excitonic features, and crystalline order.
- Infrared – Carrier concentrations, mobilities, and phonon behavior.

This versatility makes ellipsometry valuable across semiconductors, photovoltaics, and 2D materials.

Modeling: Turning Ψ and Δ into Physical Insight

One of ellipsometry's defining features is its reliance on modeling. Raw Ψ–Δ spectra contain all the necessary information about the sample. However, to extract the desired material properties, the data must be modeled using a multilayer structure that closely represents the actual sample.

Modeling typically involves:

- Defining layer structure (substrates, thin films, interfaces, roughness layers)
- Using known or estimated optical constants (n, k)
- Iteratively refining fits against measured spectra

The process can be complex, but it is precisely this step that allows ellipsometry to extract high-value information—layer thicknesses, dielectric functions, roughness, and even multi-layer film stacks. Dr. Diware noted that while modeling is sometimes seen as a barrier, it is actually a powerful interpretive tool: "If your model is accurate, it will give you insights beyond what direct measurements can show."

The Leap to Imaging Spectroscopic Ellipsometry (ISE)

Traditional ellipsometry measures an averaged response over a spot size ~50 µm or larger. For shrinking devices structures, this is a limitation: local variations are invisible.

ISE solves this by replacing the point detector with a 2D camera. Every pixel becomes a detector, providing localized Ψ and Δ values (see **Fig. 1**). Lateral resolution can reach 1 µm while vertical resolution remains at ~0.1 nm.

In practical terms, ISE can collect millions of spectra in a single scan, producing full-field maps of optical properties. This is crucial for patterned wafers, 2D materials, and non-uniform coatings.

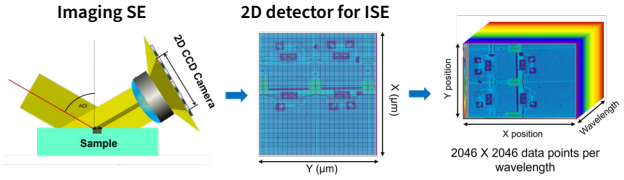

Fig. 1. *Measurement scheme of imaging spectroscopic ellipsometry employing a 2D-detector.*

Applications: From 2D Materials to Real-Time Electrochemistry

Dr. Diware highlighted several applications where ISE is transformative:

1. 2D Materials & Heterostructures

ISE excels in characterizing atomically thin materials such as MoS_2, [2, 3] WS_2, [4] and graphene [5]. By mapping Ψ–Δ pixel-by-pixel, ISE can distinguish monolayer, bilayer, and trilayer regions and extract anisotropic dielectric properties. In one example, a MoS_2 flake on 300 nm SiO_2/Si was mapped in a single field of view—substrate, flake, and thickness variations all captured simultaneously.

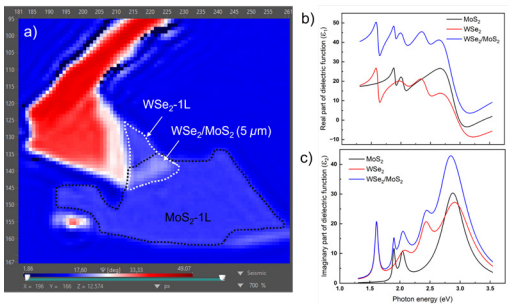

Fig. 2. *TMDC materials and their heterostructure:* **a)** *Ψ map,* **b)** *real and* **c)** *imaginary part of dielectric function for monolayer MoS_2, WSe_2 and the MoS_2/WSe_2 heterostructure.*

2. Patterned and Microstructured Surfaces

ISE can resolve optical property variations across lithographically patterned surfaces, including variations at edges and interfaces. This is vital for advanced electronics and photonics manufacturing, where uniformity at the micro-scale is critical.

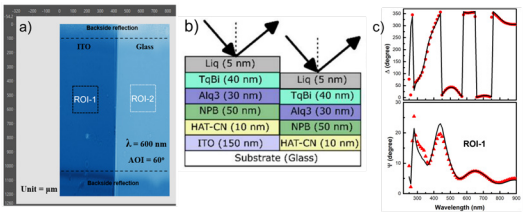

e)

Layer No.	Material	Thickness (nm)		
		Proposed (nm)	Measured (nm)	
			Glass (ROI-2)	ITO (ROI-1)
6	Liq	5	5.14	4.55
5	TpBi	40	40.10	38.72
4	Alq3	30	31.53	29.43
3	NBP	50	50.88	46.29
2	HAT-CN	10	12.38	12.52
1	ITO	150	-------	140.47
0	Glass (Substrate)	1 mm	1 mm	1mm

Fig. 3. *Organic Solar Cell (OSC) Characterization:* **a)** *Layered structure of the OSC fabricated via thermal evaporation on an ITO-patterned glass substrate.* **b)** *Ψ map illustrating regions with and without ITO.* **c)** *Ψ and* **d)** *Δ spectra extracted from ROI-1 and ROI-2, as marked in* **Fig. 3b**. **e)** *Layer thicknesses determined through multilayer optical modeling; measured values show close agreement with the proposed design.*

3. Transparent Substrates & Knife-Edge Illumination

Backside reflections pose a significant challenge when working with transparent substrates such as glass. Park Systems addresses this with a knife-edge illumination setup that blocks half the beam, eliminating backside noise. This allows accurate measurements even on low-cost substrates.

4. Ellipsometric Contrast Microscopy (ECM)

For rapid visualization, ECM mode within ISE optimizes polarizer/analyzer angles to enhance contrast of low-optical-contrast features [5]—making monolayer flakes visible even on plain glass substrates without expensive oxide-coated wafers.

5. Real-Time Monitoring of Intercalation Processes

ISE can investigate dynamic processes, such as sodium-ion intercalation in Janus graphene. **Fig. 4** shows the operando observation of Δ shifts, enables researchers to monitor ions moving in and out of layered structures in real time — providing unprecedented insight into electrochemical processes vital to energy storage [6, 7].

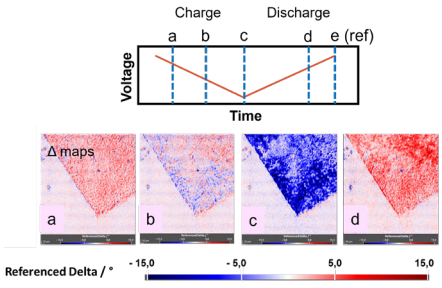

Fig. 4. *Tracking the Na+ movement into Janus graphene electrode: The Δ maps displaying the Na + intercalation/deintercalation in AB graphene during charging/discharging process.*

Technical Framework: Anatomy of an ISE System

An ISE setup includes:

- Polarizer and compensator for controlling incident polarization
- High-precision sample stage under a microscope objective
- 2D photodiode, CCD or CMOS camera for pixel-resolved detection

During measurement, the compensator is rotated, and at each step the camera captures intensity maps. From these, Ψ and Δ maps are calculated. Full-field data can be analyzed as a whole or divided into regions of interest (ROI) for targeted modeling.

In display research, for example, a single scan of a pixel cell can be subdivided into RGB subpixel regions, each modeled separately—without rescanning.

Case Study: MoS_2 Anisotropy

One striking example involved MoS_2 exfoliated onto a SiO_2/Si substrate. ISE captured the full flake in one scan. Modeling revealed strong in-plane (x-y) excitonic peaks (A and B excitons) and absence of such peaks along the out-of-plane (z-axis) direction, consistent with confinement effects. The measured birefringence exceeded 2.5—among the highest reported [3].

Such anisotropy has direct implications for integrating 2D materials into photonic devices and hybrid optoelectronic–photonic circuits.

Why ISE Matters: A Researcher's Perspective

ISE is more than just an incremental improvement in ellipsometry—it fundamentally changes the scale and nature of the analysis:

- **Non-contact & Non-destructive** – Ideal for delicate films and functional devices.
- **Vertical & Lateral Resolution** – Sub-nanometer vertical sensitivity combined with micron-scale lateral mapping.
- **Throughput & Efficiency** – Millions of spectra captured per scan, enabling rapid evaluation of complex samples.
- **Interpretive Power** – Model-based analysis transforms optical data into physical, structural, and functional understanding.

As Dr. Diware concluded, "If you have a research problem and no solution in sight, imaging ellipsometry might be the key."

Conclusion: Expanding the Reach of Optical Metrology

With Imaging Spectroscopic Ellipsometry, Park Systems is redefining what optical metrology can deliver. From single layer 2D materials to multi-layer OLED stacks, from transparent substrates to real-time electrochemistry, ISE combines precision, versatility, and efficiency.

Its capacity to map both thickness and optical properties at high lateral resolution opens entirely new avenues for understanding and engineering advanced materials.

ISE is not just the next step in ellipsometry, it is becoming an indispensable tool in the expanding frontier of nanoscience and technology.

References

1. Aspnes D.E., (2014). Spectroscopic ellipsometry – Past, Present, and future, 571 (3) 334.
2. Funke, S., Miller, B., Parzinger, E., Thiesen, P., Holleitner, A. W., & Wurstbauer, U. (2016). Imaging spectroscopic ellipsometry of MoS_2. Journal of Physics: Condensed Matter, 28(38), 385301.
3. Ermolaev, G. A., Grudinin, D. V., Stebunov, Y. V., Voronin, K. V., Kravets, V. G., Duan, J., A. B. Mazitov, Tselikov, G. I., Bylinkin, A., Yakubovsky, D. I., Novikov, S. M., Baranov, D. G., Nikitin, A. Y., Kruglov, I. A., Shegai, T., Alonso-González, P., Grigorenko, A. N., Arsenin, A. V., Novoselov, K. S., Volkov, V. S. (2021). Giant optical anisotropy in transition metal dichalcogenides for next-generation photonics. Nature Communications, 854 (12) 1.
4. Wurstbauer, U., Röling, C., Wurstbauer, U., Wegscheider, W., Vaupel, M., Thiesen, P. H., & Weiss, D. (2010). Imaging ellipsometry of graphene. Applied Physics Letters, 97(23), 231901
5. Sigger, F., Lambers, H., Katharina, N., Klein, J., Saigal, N., Holleitner, N. W., Wurstbauer, U. (2022). Spectroscopic imaging ellipsometry of two-dimensional TMDC heterostructures. Applied Physics Letters, 121 (7) 071102.
6. Sun, J., Sadd, M., Edenborg, P., Grönbeck, H., Thiesen, P. H., Xia, Z., ... & Palermo, V. (2021). Real-time imaging of Na+ reversible intercalation in "Janus" graphene stacks for battery applications. Science advances, 7(22), eabf0812.
7. Okano, S., Sharma, A., Ortmann, F., Nishimura, A., Günther, C., Gordan, O. D., ... & Zahn, D. R. (2020). Voltage-controlled dielectric function of bilayer graphene. Advanced optical materials, 8(20), 2000861.

About Dr. Mangesh Diware

Dr. Mangesh Diware is a Senior Application Scientist at Park Systems Inc., California. He holds dual master's degrees—one in Physics from Nagpur University (2006) and another in Materials Engineering from Visvesvaraya National Institute of Technology (VNIT), India (2009). He earned his Ph.D. in Physics from Kyung Hee University, South Korea, in 2014 under the guidance of Prof. Young Dong Kim. From 2014 to 2017, Dr. Diware worked as a Senior Research Scientist at the Korea Research Institute of Standards and Science (KRISS), where he focused on developing ultrathin film metrology techniques. In 2018, he joined Seoul National University as a Research Associate, conducting advanced optical spectroscopy studies on quantum materials.

With over a decade of experience in materials science and optical spectroscopy, Dr. Diware specializes in exploring material properties using light-based techniques, particularly spectroscopic and imaging ellipsometry. His work contributes to advancements in semiconductors, flexible electronics, and next-generation display technologies. His accolades include the Presidential Fellowship, a Postdoctoral Fellowship from KRISS, and the "Best Researcher of the Year" award at KRISS.

Continued from page 24:

Nanopatterning on 2D Materials: A Case Study on Graphene by AFM-Based Nanolithography

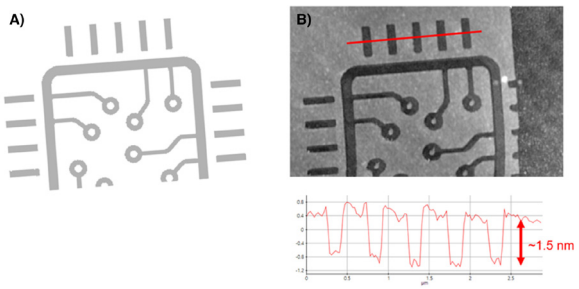

Fig. 7. *AFM result of graphene patterning from original image by the Bias mode of AFM-based nanolithography. Original image* A) *and AFM image* B).

Conclusions

This study demonstrates the effectiveness of AFM-based nanolithography, specifically the Bias mode, for achieving precise nanopatterning on a single layer of graphene. We examined two approaches for AFM-based nanolithography: the mechanical (Set Point/Z scanner mode) and chemical (Bias mode) methods. While mechanical cutting can achieve direct physical etching, it is prone to issues such as unintended damage to the surrounding graphene. The Bias mode, however, proved to be more favorable for graphene nanopatterning due to its ability to induce controlled oxidation using an electric field, thus minimizing physical stress on the AFM tip and allowing for smoother, more precise cuts. Through systematic exploration of key parameters—including applied bias, AFM tip approach speed, and humidity conditions—we identified optimal settings for controlled graphene cutting.

These results contribute to a deeper understanding of AFM-based nanolithography on graphene, providing a practical framework for optimizing parameters to achieve high-fidelity patterns. These insights support the development of advanced graphene applications in nanoelectronics, sensors, and other fields requiring high-resolution patterning.

References

1. Geim, A. K. (2009). Graphene: status and prospects. science, 324(5934), 1530-1534.
2. Li, X., Yu, J., Wageh, S., Al-Ghamdi, A. A., & Xie, J. (2016). Graphene in photocatalysis:` a review. Small, 12(48), 6640-6696.
3. Tiwari, S. K., Sahoo, S., Wang, N., & Huczko, A. (2020). Graphene research and their outputs: Status and prospect. Journal of Science: Advanced Materials and Devices, 5(1), 10-29.
4. Albisetti, E., Petti, D., Pancaldi, M., Madami, M., Tacchi, S., Curtis, J., ... & Bertacco, R. (2016). Nanopatterning reconfigurable magnetic landscapes via thermally assisted scanning probe lithography. Nature nanotechnology, 11(6), 545-551.
5. Wei, Z., Wang, D., Kim, S., Kim, S. Y., Hu, Y., Yakes, M. K., ... & Riedo, E. (2010). Nanoscale tunable reduction of graphene oxide for graphene electronics. Science, 328(5984), 1373-1376.
6. https://www.parksystems.com/en/products/research-afm/AFM-modes/Nanomechanical-Modes/nanolithography
7. https://www.parksystems.com/en/products/research-afm/small-sample-afm/nx10
8. Vincenti, L., Pellegrino, P., Cascione, M., De Matteis, V., Farella, I., Quaranta, F., & Rinaldi, R. (2024). Crafting at the nanoscale: A comprehensive review of mechanical Atomic force microscopy-based lithography methods and their evolution. Materials & Design, 113036.
9. Li, H., Ying, Z., Lyu, B., Deng, A., Wang, L., Taniguchi, T., ... & Shi, Z. (2018). Electrode-free anodic oxidation nanolithography of low-dimensional materials. Nano letters, 18(12), 8011-8015.
10. Chua, C. K., & Pumera, M. (2014). Chemical reduction of graphene oxide: a synthetic chemistry viewpoint. Chemical Society Reviews, 43(1), 291-312.
11. Arif, T., Colas, G., & Filleter, T. (2018). Effect of humidity and water intercalation on the tribological behavior of graphene and graphene oxide. ACS applied materials & interfaces, 10(26), 22537-22544.

Microscopic Thin Film Metrology and Visualization

Empower your research with our next-generation Imaging Ellipsometer

Accurion EP4

The Accurion EP4 is our latest generation of imaging ellipsometers that combines ellipsometry and microscopy. This enables the characterization of thickness and refractive index with the sensitivity of ellipsometry on micro-structures as small as 1 μm. The microscopic part enables a simultaneous measurement of all structures inside the field of view of the optical system.

- High lateral ellipsometric resolution for thickness and refractive index on microstructures as small as 1 μm.
- Intuitive region selection through drawing in the live ellipsometric view before measurement.
- Continuous spectroscopic imaging ellipsometry from UV to NIR.
- Expanded application of ellipsometry to small structures with new features and accessories.

Park SYSTEMS

parksystems.com/ep4

PUSHING THE LIMITS: DEEPER INSIGHTS IN PFM AND A NEW DIMENSION IN MFM

Prof. Dr. Lukas M. Eng, Institute of Applied Physics, TU Dresden, Germany
Adapted from Presentation, Edited by NanoScientific

Introduction

At the 2024 NanoScientific Forum Europe in Munich, Prof. Dr. Lukas M. Eng brought the audience back to two of the most established techniques in scanning probe microscopy—Piezoresponse Force Microscopy (PFM) and Magnetic Force Microscopy (MFM)—only to show how both are being pushed far beyond their traditional limits.
For more than thirty years, these techniques have been the workhorses for imaging ferroelectric and magnetic domains at the nanoscale. But Prof. Eng's latest work at TU Dresden demonstrates how careful experimental design and theoretical modeling can expand what these methods can do. In PFM, his group has been asking a deceptively simple question: how far into a material can PFM "see" beneath the surface? And in MFM, they are extending the method from its classic out-of-plane sensitivity into a true three-dimensional probe of magnetic fields.
The results redefine the boundaries of both techniques—turning PFM into a quantitative volumetric probe and MFM into a multidimensional magnetic field mapping tool.

PFM: Looking Beneath the Surface

PFM has long been a go-to technique for visualizing ferroelectric domain structures. Since its origins in the early 1990s, when K. Franke first demonstrated voltage-modulated scanning force microscopy [1], the method has been refined and expanded. Prof. Eng himself played a key role in this evolution, introducing in-plane PFM in 1998 [2] and full three-dimensional PFM the following year [3].

Yet despite decades of use, one fundamental question persisted: when we apply an AC bias to the tip in PFM, what is the actual volume of the material we are probing? Most PFM measurements are interpreted as surface-sensitive, but there have been hints for years that the electric field penetrates far into the bulk. Quantifying that penetration depth has been a long-standing challenge.

Earlier efforts provided glimpses of the answer. In 2009, Johann and co-workers showed that in lithium niobate, measurable PFM signals could be detected to depths of roughly 1.7 microns [4]. In 2019, Steffes et al. introduced tomographic PFM [5], physically milling away the sample layer by layer to correlate PFM signals with depth. While effective, the method was destructive and impractical for most applications.

Prof. Eng's group sought a different path [6]: a way to measure the effective probing depth (see **Fig. 1**) of PFM quantitatively, without damaging the sample.

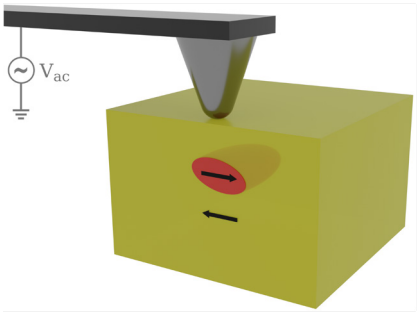

Fig. 1. *PFM principle for probing polar information into the depth of a sample.*

The work was led by Ph.D. candidate Matthias Roeper, who developed a theoretical model describing how the AC electric field applied by the PFM tip penetrates into a dielectric. In an idealized scenario, with no free charges, the field could extend indefinitely into the bulk. In reality, geometry matters. The model showed that solely the tip radius and the signal-to-noise performance of the instrument defines the effective probing depth and depth resolution. The model as shown in **Fig. 2**, predicts that the PFM signal is at its maximum close to the sample surface, then reaches a zero-amplitude value at a depth equal to the tip radius, before recovering into the sample depth. The 90-percent depth – defined as 90-percent of the initial normalized PFM amplitude signal at the sample surface – is achieved at nineteen times the tip radius. This 90-percent probing depth can be used to estimate the effective probing depth for standard PFM cases in a much simpler way, rather than applying the full calculation using a multi-parameter model.

Testing the model experimentally required a carefully prepared sample. The group chose x-cut periodically-poled lithium niobate (PPLN), a crystal whose domains are polarized in-plane (see **Fig. 2**). By embedding the crystal in epoxy and polishing it at a shallow wedge of about three degrees, they created a surface where domain boundaries appeared at progressively greater depths along the scan direction. This allowed the PFM tip to encounter increasing depths in a single scan.

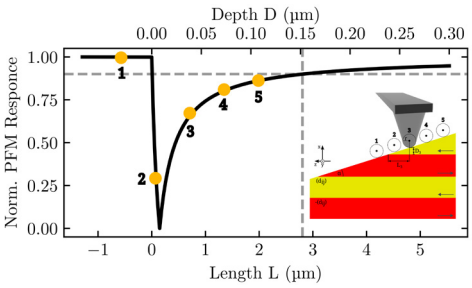

Fig. 2. *x-cut $LiNbO_3$ wedge sample (inset) used to quantify PFM penetration depth [6]. The PFM signal reaches a minimum (between measurements 2 and 3) and then recovers; in this case, probing to a depth of 150 nm is possible.*

The results aligned strikingly with the model. The PFM amplitude showed a sharp change when the tip reached a depth equal to its radius, and then recovered hyperbolically as the depth increased. The 90-percent probing depth matched the predicted nineteen times of the tip radius. For a typical 60-nanometer platinum-coated tip, the method could non-destructively probe more than one micron into the sample.

One of the strengths of the model was its robustness. The team systematically varied the AC voltage from one to above eight volts, changed the drive frequency between resonance and off-resonance conditions, and altered the contact force from light to heavy. None of these changes affected the measured depth. Only the tip radius mattered—a simple but powerful insight.

Prof. Eng emphasized one important caveat for researchers working on thin films and two-dimensional materials. In ultrathin samples, the PFM field penetrates well beyond the active layer into the substrate. The measured signal will therefore include contributions from the substrate, making it essential to account for substrate properties when interpreting PFM data from van der Waals ferroelectrics or oxide heterostructures.

MFM: Adding a New Dimension

While the advance in PFM focuses on looking deeper into a material, the innovation in MFM aims to look in more directions at once.

Conventional MFM is typically performed in vertical mode (i.e. VMFM), in which the cantilever oscillates in its flexural mode to detect the out-of-plane component of the magnetic stray field above a sample (see **Fig. 3a**). This works well for simple ferromagnetic domain structures, such as those in a hard disk, but it captures only part of the picture. In modern magnetic materials—particularly those hosting topological spin textures such as skyrmions and antiskyrmions—the in-plane components of the stray field are equally important for understanding the underlying physics.

Prof. Eng's group set out to extend MFM into three dimensions by measuring both the vertical and lateral components of the magnetic field (see **Fig. 3a**). This work, led by Bachelor's student Jori Schmidt and supervised by postdoc Sam Seddon, involved exciting the cantilever in both its flexural and torsional resonances simultaneously [7]. The flexural resonance captures the vertical component (MFM or VMFM) while the torsional resonance captures the in-plane components (LMFM). With separate piezo excitations and lock-in amplifiers for each mode, both signals can be collected at once.

Testing the approach on a hard disk with well-defined perpendicular magnetic domains provided a clear proof of concept (**Fig. 3**). In VMFM mode, the alternating up and down magnetization of the domains produced the expected stripe contrast. In LMFM mode, strong contrast appeared only when the torsional oscillation was perpendicular to the domain walls (see **Fig. 3b,c**), whereas the contrast disappeared when the oscillation was aligned parallel to the walls. This matched the expected magnetic symmetry, and confirmed that LMFM was selectively detecting the appropriate in-plane field components.

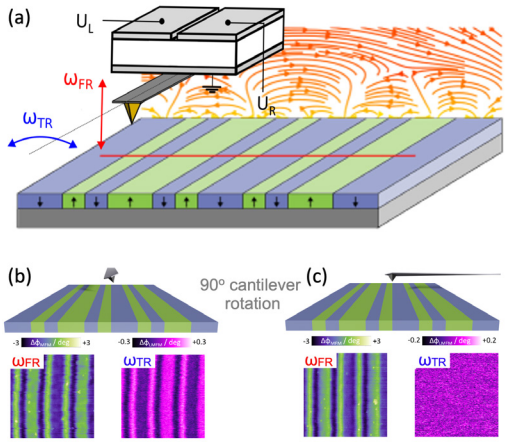

Fig. 3. a) *VMFM and LMFM implemented via a split piezo-shaker operating simultaneously at ω_FR and ω_TR for resonant flexural and torsional excitation. LMFM was tested on a magnetic hard disk [7]; the magnetic stray field shows appreciable in-plane gradients that LMFM can detect.* **b,c)** *VMFM and LMFM responses from the same hard disk with cantilever torsion aligned perpendicular* **b)** *and parallel* **c)** *to the domain walls. In case* **c)**, *the LMFM signal is absent because no in-plane stray field component is present for the tip to couple with.*

To validate the interpretation, the group modeled the MFM tip as a magnetic point dipole using the magpylib simulation package. The simulated stray fields produced VMFM and LMFM contrasts in close agreement with the experimental measurements, including the phase inversion between the vertical and lateral signals. Small discrepancies for LMFM when the torsional oscillation was parallel to the domain walls were attributed to subtle tip–sample coupling effects, which will be explored in future refinements.

The significance of 3D MFM becomes clear in more complex materials. Prof. Eng's group has already started to apply this technique to MnPtPdSn samples, which host antiskyrmion lattices at room temperature. These topological spin textures cannot be fully understood without measuring both vertical and in-plane components of the stray field. By thinning lamellae to around two microns and mounting them free-standing, the group could perform 3D MFM to capture the complete stray field distribution.

Conclusion: Extending the Reach of Scanning Probe Microscopy

In PFM, Prof. Eng's group has transformed the question of depth from a vague concept into a quantitative, non-destructive measurement directly linked to the tip radius and the instrument's performance. In MFM, they have expanded the technique into a true three-dimensional probe capable of revealing complex magnetic field distributions.

These developments will have broad implications for researchers working in (multi-)ferroic materials, where functionality often depends on structures buried below the surface or on the interplay of multiple field components. Prof. Eng's work serves as a reminder that even well-established techniques can be extended to new frontiers when carefully examined.

As he told the NanoScientific Forum Europe audience, "In PFM, remember the substrate. In MFM, remember the other components of the field." It is a fitting summary of an approach that balances experimental precision with physical insight—pushing the limits of scanning probe microscopy into deeper and more multidimensional territory.

About Prof. Dr. Lukas Eng

Dr. Lukas M. Eng is a Full Professor at the Excellence-University "Technische University Dresden (TUD), Germany". His focus lies on experimentally exploring the nanoscale magnetic, electronic, and optical properties of modern-type low-dimensional and/or topological materials, by applying various scanning-probe-microscopy-based methods at room and low temperatures. Special focus is laid to explore frustrated nanomagnetic systems that show non-collinear magnetic spin textures such as skyrmions, as well as photon-polaritons in layered and twisted 2D materials. He received a PhD and venia legendi from the University of Basel, Switzerland, while then was hired as a full-professor at TUD after several post-doctoral experiences, nominally in Molecular Electronic Devices (BASF AG, Germany), Biophysics (Univ. Geneva, CH), and Nonlinear and Quantum Optics (ETH Zürich, CH). He has published over 400 peer-reviewed articles in the fields of nanooptics, nanoelectronics, non-collinear magnetic nanostructures, linear and nonlinear optics, biophysics, and others more: *Details can be found at: https://tu-dresden.de/mn/physik/iapp/experimentalphysik-photophysik#intro.*

References

1. K. Franke, L.M. Eng, M. Weihnacht, W. Haessler, and J. Besold
   The creation of the piezoresponse force microscopy twenty-three years ago IEEE Intern. Symp. Appl. Ferroelectr. & Europ. Conf. Appl. Polar Dielectr. and Piezoelectric Force Microscopy Workshop (ISAF/ECAPD/PFM), 1 (2016); https://doi.org/10.1109/ISAF.2016.7578100.
2. M. Abplanalp, L. Eng, and P. Günter
   Mapping the Domain Distribution at Ferroelectric Surfaces by Scanning Force Microscopy
   Appl. Phys. A 66, S231 (1998); https://doi.org/10.1007/s003390051136.
3. L.M. Eng, H.-J. Güntherodt, G.A. Schneider, U. Köpke, and J. Muñoz Saldaña, Nanoscale Reconstruction of Surface Crystallography from 3-Dimensional Polarization Distribution in Ferroelectric Barium-titanate Ceramics Appl. Phys. Lett. 74, 233 (1999); https://doi.org/10.1063/1.123266.
4. F. Johann, Y. J. Ying, T. Jungk, Á. Hoffmann, C. L. Sones, R. W. Eason, S. Mailis, and E. Soergel, Depth resolution of piezoresponse force microscopy, Appl. Phys. Lett. 94, 172904 (2009);
5. J.J. Steffes, R.A. Ristau, R. Ramesh, and B.D. Huey,
   Thickness scaling of ferroelectricity in BiFeO3 by tomographic atomic force microscopy, Proc. Natl. Acad. Sci. U.S.A. 116, 2413–2418 (2019);
6. M. Roeper, S.D. Seddon, Z.H. Amber, M. Rüsing, and L.M. Eng
   Depth resolution in piezoresponse force microscopy J. Appl. Phys. 135, 224102 (2024); https://doi.org/10.1063/5.0206784.
7. J. Schmidt, L.M. Eng, and S.D. Seddon
   Towards 3D Magnetic Force Microscopy: Simultaneous torsional cantilever excitation to access a second, orthogonal stray field component J. Appl. Phys. 136, 113904 (2024); https://doi.org/10.1063/5.0226570.

IMAGING FORBIDDEN LIGHT: NANO-SPECTROSCOPY OF POLARITONS IN 2D OXIDE MEMBRANES

Prof. Alex McLeod, University of Minnesota
Adapted from Presentation, Edited by NanoScientific

Introduction: Probing the Hidden Realm of Light and Matter

At the 2024 NanoScientific Symposium Americas, Prof. Alex McLeod of the University of Minnesota invited attendees into a very different vision of optical microscopy—one that ventures deep into a regime traditional optics cannot reach. His focus was on polaritons—hybrid light–matter excitations that live in the so-called "forbidden light" region—and on the technique capable of imaging them: **scattering-type scanning near-field optical microscopy (s-SNOM)**.

In this "zone of forbidden light," near-field optical techniques make visible what far-field optics cannot. Polaritons not only provide a window into the quantum properties of materials, but can also be engineered and manipulated for advanced photonic applications. Prof. McLeod's research reveals how these exotic excitations propagate, interact, and even refract in **man-made 2D oxide membranes (Fig. 1)**.

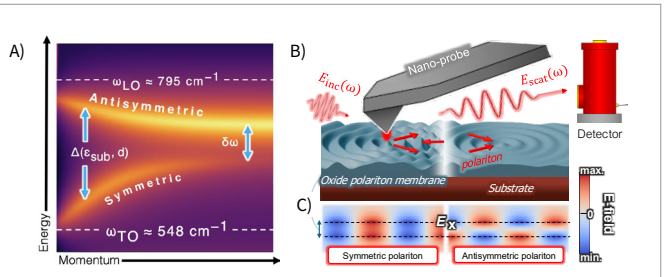

Fig. 1. A) *Phonon polaritons in $SrTiO_3$ membranes are hybrid modes of light and lattice vibrations. Coupling across the membrane's top and bottom interfaces forms symmetric and antisymmetric modes with tunable positive or negative dispersion of energy (ω) versus momentum ($q \propto \lambda$, where λ is the polariton wavelength).* B) *Near-field microscopy uses a sharp, metal-coated probe illuminated by an infrared laser to launch and detect polaritons by scattering their evanescent fields to a detector. Veselago lensing occurs when symmetric polaritons enter a region with negative dispersion.* C) *The internal distribution of oscillating charges and lateral electric fields (e.g., Ex) determines the mode symmetry.*

Quantum Materials: Why Resolution Matters

Prof. McLeod's scientific motivation begins with a broad category: **quantum materials**—systems in which interactions between electrons, or between electrons and the crystal lattice, dominate their physical behavior. This interaction-driven complexity produces emergent phenomena such as insulator–metal transitions in oxides like VO_2, driven by temperature or external fields; high-temperature superconductivity, often competing with charge-ordered phases; topological edge states with spin-selective conduction; and designer quantum phases, such as twisted bilayer graphene that hosts superconductivity at "magic" angles.

However, these phenomena are **spatially heterogeneous**. Domains form, percolate, and compete at nanometer scales. Averages over microns or millimeters miss these fine details.

This is where high-resolution scanning probe techniques—AFM, STM, and in Prof. McLeod's case, near-field optical spectroscopy—become essential. They not only resolve local properties but can **optically map phase coexistence and transitions in real space**.

Beating the Abbe Limit: Why Forbidden Light Matters

For optical scientists, the **Abbe diffraction limit** has long been a barrier: the smallest resolvable feature in conventional optics is proportional to the wavelength of light. For the mid-infrared light Prof. McLeod uses to probe low-energy excitations, that limit is on the order of microns—far too coarse for nanoscale physics.

The solution is to enter the **near field**. A sharp, metalized AFM tip is illuminated with infrared light, acting as a nanoscopic antenna that localizes the field at its apex. The sample's response is encoded in evanescent waves—non-propagating fields confined to nanometer distances from the surface. These near-field signals are scattered by the tip into the far field, where they can be collected by a detector.

This approach lets Prof. McLeod **image "forbidden light"**—evanescent modes, including polaritons, that cannot be accessed with standard far-field optics.

Polaritons: Hybrid Waves of Light and Matter

The stars of Prof. McLeod's work are **polaritons**—mixed modes that combine electromagnetic waves with material excitations. Depending on the host material, these can include:

- **Plasmon polaritons** (light coupled to free electron oscillations)
- **Phonon polaritons** (light coupled to lattice vibrations)
- **Exciton polaritons** (light coupled to bound electron–hole pairs)
- **Magnon polaritons** (light coupled to spin waves)

In all cases, polaritons compress the wavelength of light, sometimes by factors of 100 or more, allowing them to propagate and interact at scales ideally suited for nanophotonics.

Because they live in the near field, polaritons are **highly confined** and **long-lived**—immune to direct radiation loss into free space unless scattered by edges or defects. This makes them excellent candidates for **on-chip guiding, focusing, and sensing**.

Polariton Interferometry: Measuring Wavelength and Lifetime

To characterize polaritons, Prof. McLeod's team uses **interferometric mapping**. The AFM tip launches polaritons into the material, where they propagate until reflecting from an edge or interface. The forward and reflected waves interfere, producing a standing wave pattern.

By scanning the tip toward and away from an edge, Prof. McLeod records interference fringes. From these fringes, the **polariton wavelength** and **propagation length** (related to the quality factor Q) can be extracted.

In high-quality graphene encapsulated in hexagonal boron nitride, for example, Q-factors can exceed 50–100 at low temperature. In oxide membranes, current Q-factors are lower (~3) due to scattering, but the technique remains the most direct way to study polariton behavior.

Moving Beyond Graphene: Why Oxide Membranes?

Graphene has been a showcase for plasmon polaritons, but Prof. McLeod's current interest is in **transition metal oxides**, particularly **strontium titanate ($SrTiO_3$)**. Like other so-called perovskite oxide crystals, $SrTiO_3$ showcases ferroelectricity - or "switchable" macroscopic electric polarization – but also more exotic behaviors like unconventional su-

perconductivity at low temperature.

These oxides are grown by **molecular beam epitaxy (MBE)** onto sacrificial buffer layers. Using **remote epitaxy**, the oxide film can then be peeled from the growth substrate and transferred as a **free-standing membrane** onto almost any target substrate. **Prof. Bharat Jalan** at University of Minnesota, Prof. McLeod's chief collaborator, has pioneered **hybrid MBE** techniques to grow a wide assortment of oxides in membrane form. This opens new frontiers for nanoelectronics and nanophotonics based entirely on quasi-2D oxides.

These materials offer several advantages, including custom thicknesses ranging from a few to tens of nanometers, bulk-like crystallinity even at small thicknesses, and the ability to tailor substrate environments to control polariton dispersion. They also exhibit switchable phases such as ferroelectricity, which are not easily achieved in conventional 2D materials. Additionally, oxides like $SrTiO_3$ host strong infrared-active phonons, making them ideal for phonon polariton generation and manipulation.

Hyperspectral Nano-Imaging: Mapping Polaritons in Action

Using a Park Systems NX10 AFM coupled with a **tunable pulsed laser** (via optical parametric amplification), Prof. McLeod performs **hyperspectral nano-FTIR imaging**.

This system combines:

- **Broadband frequency coverage** for phonon resonances
- **Michelson interferometer** for phase-resolved detection
- **Tapping mode operation** for simultaneous AFM and optical mapping

In $SrTiO_3$ membranes, the team images **phonon polariton fringes** emanating from edges. By tuning the laser frequency, they record the **dispersion relation**—how the polariton wavelength changes with frequency **(Fig. 1A)**.

This measurement directly confirms the presence of **propagating phonon polaritons (Fig. 2A-B)** and matches theoretical models based on the membrane thickness and dielectric environment.

Two-Branch Polariton System: Symmetric and Antisymmetric Modes

A key discovery is that oxide membranes support **two polariton modes**. Each surface (top and bottom) can host a surface polariton. When the two interact, they form:

- **Symmetric (bonding) mode** with positive group velocity
- **Antisymmetric (antibonding) mode** with negative group velocity

Fig. 1C shows the predicted electric field profile of these interfacially coupled hybrid polariton modes. The separation between these modes is a **Rabi splitting Δ** proportional to their mutual coupling strength, measured directly in **Fig. 2C**.

The **opposite group velocities** are particularly intriguing. Negative group velocity polaritons open the door to **negative refraction**, or **Veselago lensing**—where polariton waves focus beyond a lens without diffraction **(Fig. 1B)**.

Veselago Lensing in Membranes

By engineering suspended and supported regions of the membrane, Prof. McLeod can spatially control polariton dispersion.
In one configuration:

- **Suspended region** supports propagating modes
- **Supported region** creates a polaritonic "bandgap"

A polariton launched from a point source in the suspended region can refract negatively at the interface, focusing into a sharp image in the supported region.

This **on-chip Veselago lens** could form the basis for **polariton optics devices**, enabling subwavelength focusing and imaging.

Instrumentation: A Platform for Forbidden Light

The experiments require a carefully integrated system built upon a Park Systems scanned probe microscope:

- **Park Systems NX10 AFM** for stable tapping-mode near-field operation
- **Parabolic mirror + retroreflector** for focusing illumination and collecting scattered light
- **Michelson interferometer** for phase and amplitude separation
- **Broadband tunable pulsed laser** covering mid-infrared phonon energies
- **Cryogenic stage** for low-temperature measurements (down to 15 K) to improve Q-factors

The setup allows simultaneous **topography, optical maps, and electrical potential mapping**—enabling true multi-modal characterization of quantum materials.

Challenges and Future Directions

Current polariton Q-factors in oxide membranes are modest, limited by scattering from imperfections. Improving **MBE growth, membrane transfer,** and **surface quality** will help.

Cryogenic measurements are expected to extend propagation lengths significantly. Combined with membrane engineering (thickness, substrate tuning), this will open the way to **on-chip polariton waveguides, resonators, and logic circuits**.

Conclusion: A New Kind of Optics for Quantum Materials

Prof. Alex McLeod's work marks a shift in optical microscopy—from imaging surfaces to imaging the light trapped within them. By mapping polaritons in 2D oxide membranes, his team is developing a powerful platform for mid-infrared nanophotonics, potentially transforming how we sense, process, and control quantum materials at the nanoscale. These hybrid light–matter waves not only reveal hidden optical behavior but also open practical pathways toward compact, chip-scale devices for spectroscopy, sensing, and photonic computation.

As he told the NSFA audience: "We're not just imaging materials anymore. We're imaging their forbidden light—and in doing so, opening entirely new dimensions of control over quantum matter."

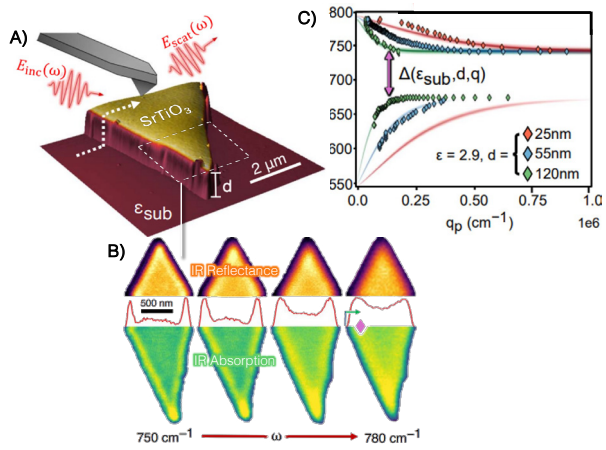

Fig. 2. A) *Height map of a tapered $SrTiO_3$ membrane imaged by infrared near-field microscopy.* B) *Scattered light reveals enhanced evanescent fields (top) and infrared absorption (bottom) at the membrane edge, indicating reflection of a probe-launched polariton with a wavelength that disperses with laser excitation energy (ω), as shown by polariton line profiles (red curves). The field crest (e.g., marked by the diamond symbol) defines the polariton wavelength and thus its momentum q versus ω. Dispersion of symmetric and antisymmetric modes and their Rabi splitting Δ are tunable by membrane thickness* C) *and substrate permittivity (ε_sub). When ε_sub varies spatially, positively and negatively dispersing polaritons can coexist at the same ω, enabling transformation optics and Veselago lensing within a single membrane.*

About Prof. Alex McLeod

Dr. Alex McLeod is an Assistant Professor in the School of Physics and Astronomy at the University of Minnesota, where he leads research in nano-optical spectroscopy and quantum materials. He earned his Ph.D. in Physics with honors from the University of California, San Diego, and completed postdoctoral work at Columbia University as a Director's Fellow with the Columbia Nano Initiative.

His research explores phase transitions in quantum matter and the opto-electronic properties of next-generation 2D materials, including graphene and van der Waals heterostructures. Dr. McLeod designs and builds advanced near-field optical instruments—often operating at cryogenic temperatures—to probe light–matter interactions at the nanoscale. By combining precision experiments with theoretical analysis, his work has advanced understanding in low-temperature polaritonics and non-destructive nanospectroscopy, including contributions to NASA-supported sample analysis missions. Prof. McLeod is recipient of the 2022 International Union for Pure and Applied Physics (IUPAP) Young Faculty Award for his studies of polaritons and nanoscale phase transitions at low temperatures.

McLeod Nano-Optics & Photonics Lab. Prof. McLeod (wearing hat).

References

1. Lukaskawcez, B.; Varshney, S.; Choo, S.; Park, S. H.; Seo, D.; Thompson, L.; Hirshberg, N.; Garber, M.; Uram, D.; Binger, H.; Koester, S.; Oh, S.-H.; Low, T.; Jalan, B.; McLeod, A. Interfacial Strong Coupling and Negative Dispersion of Propagating Polaritons in Freestanding Oxide Membranes. arXiv June 27, 2025.
2. Qazilbash, M. M.; Brehm, M.; Chae, B. G.; Ho, P. C.; Andreev, G. O.; Kim, B. J.; Yun, S. J.; Balatsky, A. V.; Maple, M. B.; Keilmann, F.; Kim, H. T.; Basov, D. N. Mott Transition in VO2 Revealed by Infrared Spectroscopy and Nano-Imaging. Science 2007, 318 (5857).
3. Chen, X.; Hu, D.; Mescall, R.; You, G.; Basov, D. N.; Dai, Q.; Liu, M. Modern Scattering-Type Scanning Near-Field Optical Microscopy for Advanced Material Research. Advanced Materials 2019, 31 (24).
4. Novotny, L. Optics InfoBase: Journal of the Optical Society of America A - Allowed and Forbidden Light in near-Field Optics. I. A Single Dipolar Light Source. Josa a 1997, 14 (1), 91–104.
5. Basov, D. N.; Fogler, M. M.; García De Abajo, F. J. Polaritons in van Der Waals Materials. Science 2016, 354 (6309).
6. Fei, Z.; Rodin, A. S.; Andreev, G. O.; Bao, W.; McLeod, A. S.; Wagner, M.; Zhang, L. M.; Zhao, Z.; Thiemens, M.; Dominguez, G.; Fogler, M. M.; Castro Neto, A. H.; Lau, C. N.; Keilmann, F.; Basov, D. N. Gate-Tuning of Graphene Plasmons Revealed by Infrared Nano-Imaging. Nature 2012, 486 (7405).
7. Ni, G. X.; McLeod, A. S.; Sun, Z.; Wang, L.; Xiong, L.; Post, K. W.; Sunku, S. S.; Jiang, B. Y.; Hone, J.; Dean, C. R.; Fogler, M. M.; Basov, D. N. Fundamental Limits to Graphene Plasmonics. Nature 2018, 557 (7706), 530–533.
8. Varshney, S.; Choo, S.; Thompson, L.; Yang, Z.; Shah, J.; Wen, J.; J. Koester, S.; Andre Mkhoyan, K.; S. McLeod, A.; Jalan, B.; Koester, S. J.; Mkhoyan, K. A.; McLeod, A. S.; Jalan, B. Hybrid Molecular Beam Epitaxy for Single-Crystalline Oxide Membranes with Binary Oxide Sacrificial Layers. ACS Nano 2024, 18 (8), 6348.
9. Steinle, T.; Mörz, F.; Steinmann, A.; Giessen, H. Ultra-Stable High Average Power Femtosecond Laser System Tunable from 133 to 20 Mm. Optics Letters 2016, 41 (21).
10. Lewin, M.; Baeumer, C.; Gunkel, F.; Schwedt, A.; Gaussmann, F.; Wueppen, J.; Meuffels, P.; Jungbluth, B.; Mayer, J.; Dittmann, R.; Waser, R.; Taubner, T. Nanospectroscopy of Infrared Phonon Resonance Enables Local Quantification of Electronic Properties in Doped SrTiO3 Ceramics. Advanced Functional Materials 2018, 28 (42), 1802834.
11. Huth, F.; Govyadinov, A.; Amarie, S.; Nuansing, W.; Keilmann, F.; Hillenbrand, R. Nano-FTIR Absorption Spectroscopy of Molecular Fingerprints at 20 Nm Spatial Resolution. Nano Letters 2012, 12 (8), 3973–3978.

UTILIZING HIGH-THROUGHPUT AND HIGH-RESOLUTION AUTOMATED 3D-AFM FOR CD MEASUREMENT AND TRENCH SIDEWALL CHARACTERIZATION

Dr. Nithi Atthi, Thai Microelectronics Center (TMEC), National Science and Technology Development Agency (NSTDA), Thailand
Adapted from Presentation, Edited by NanoScientific

Intro: Precision Metrology for a New Era of Power Devices

At the 2024 NanoScientific Symposium, Dr. Nithi Atthi from the Thai Microelectronics Center (TMEC), the organization under National Science and Technology Development Agency (NSTDA), Thailand, spotlighted a pivotal transformation underway in the semiconductor industry—one driven by the explosive demand for AIoT devices, electric vehicles, and the next generation of power electronics. Central to this shift is silicon carbide (SiC), a wide bandgap semiconductor rapidly replacing traditional silicon with high-power and high-efficiency devices.

As the industry transitions from planar structures to advanced trench-based architectures for higher voltage ratings—often exceeding 1200 to 3000 volts—the fabrication challenge intensifies. Optimizing trench geometry, minimizing electric field concentration at corners, and ensuring smooth, low-roughness sidewalls have become critical steps for performance and reliability.

This is where advanced metrology becomes essential. Atomic Force Microscopy (AFM), especially in automated 3D configurations, has emerged as a uniquely capable tool to measure critical dimensions (CD), trench profiles, and sidewall roughness at nanoscale resolution—parameters that directly determine device yield, leakage current, and long-term stability and reliability.

Dr. Atthi's presentation focused on the deployment of fully automated 3D-AFM (Park NX-3DM) for high-throughput, high-accuracy trench characterization from Park Systems in SiC and silicon-based power devices applications. His work demonstrates not only the measurement capability but also the process optimization insights that can be extracted from precise 3D profiling.

From Planar to Trench: Why SiC Devices Demand 3D Metrology

Traditional power devices were predominantly fabricated in planar geometries, where the source, gate, and drain regions were defined along a flat surface. While effective for moderate voltages, this design faces limitations as voltage demands escalate for EV inverters, renewable energy systems, and industrial power electronics.

Trench structures—etched vertically into the substrate—allow a shorter channel length and conduction path reducing current crowding at the surface, lower on-resistance, and improved channel mobility. SiC in particular enables narrower trench widths to allow tighter cell pitch, and higher channels densities in the same area, further increasing performance.

However, these advantages come with engineering challenges. The bottom of the trench, if etched with a sharp radius, can concentrate electric fields, create premature breakdown points and compromising device lifetime as shown in Fig. 1. Similarly, excessive sidewall roughness can serve as a leakage pathway. The trench profile—shape, corner radius, and smoothness—must be carefully optimized through etch chemistry and post-processing such as oxidation and annealing.

This demands metrology that can quantify:

- **Trench geometry** (width, depth, angle)
- **Corner curvature** at the trench bottom
- **Sidewall and bottom roughness** at sub-nanometer levels
- **Critical dimensions (CD)** at top, middle, and bottom of the trench

AFM, especially when configured for sidewall access, is one of the few techniques capable of providing this complete set of measurements with the required resolution.

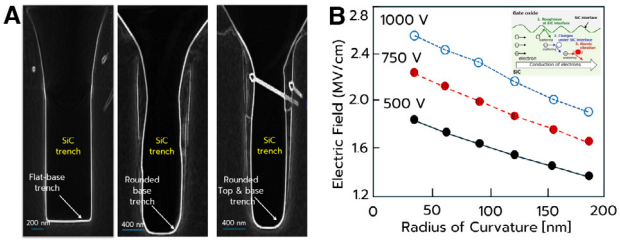

Fig. 1. A) *Example of SiC trench etched profiles comprises of flat-base trench, rounded base trench, and rounded top & base trench, and* **B)** *effects of radius of curvature of the bottom of the trench to the electric field of SiC power device.*

Automated 3D-AFM: A Metrology Platform for Production

Dr. Atthi introduced the Park NX-3DM, a fully automated AFM system designed for semiconductor production lines. Unlike laboratory AFMs used for research, the NX-3DM integrates with semiconductor fab workflows, supporting 6-inch, 8-inch, and 12-inch wafers with SEMI-standard SMIF or FOUP material handling.

Key features include:

- **Automation:** Robotic wafer handling, pre-alignment, and recipe-driven measurement sequences.
- **Non-contact scanning:** Minimizes tip wear and sample damage, critical for repetitive measurements.
- **Automatic tip exchange and tuning:** Ensures consistent performance and minimizes downtime.
- **Tilting scanning head:** Allows rotation of the Z-axis to ±19° or ±38° for direct sidewall measurement.
- **High aspect ratio tips:** Enables probing deep, narrow trenches without profile distortion.

These capabilities make the NX3DM particularly suited for trench characterization where CD uniformity, profile control, and sidewall roughness all influence device reliability.

Measuring the Sidewalls: Overcoming Conventional AFM Limitations

Conventional AFM excels at measuring flat surfaces, making it suitable for top and bottom roughness measurements. However, sidewalls—especially vertical or near-vertical surfaces and the surface roughness at the bottom of the deep trench structure—are inaccessible to a standard AFM tip scanning in perpendicular approach mode.

The Park NX-3DM addresses this with its tilting head mechanism, allowing the tip to be angled towards the trench sidewalls. By scanning at +19° and -19° tilts, the system captures height data for left and right

sidewalls. Combined with a normal (0°) scan for top and bottom surfaces, these three datasets are computationally stitched into a full 3D reconstruction of the deep trench structure.

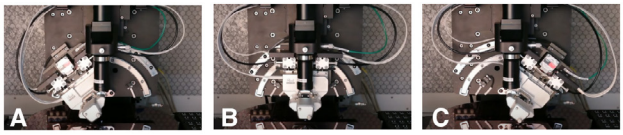

Fig. 2. *The tilting head mechanism with motorized Z-angle of Park 3D-AFM model NX-3DM* **A)** *Left-side tilting scan (maximum tilting angle of -38°),* **B)** *normal angle scan (0°), and* **C)** *Right-side tilting scan (maximum tilting angle of +38°).*

This stitched profile allows precise extraction of:

- **Top, middle, and bottom CD values**
- **Sidewall angles**
- **Sidewall roughness at specified height intervals** (e.g., 20–40% and 60–80% of trench height)
- **Corner curvature radius at trench bottom**
- **Sidewall roughness at the bottom surface of the deep trench**

The measurement repeatability is excellent, with depth and CD deviations of less than 1% from design values, and sidewall angle repeatability within 0.3°.

Demonstration: Process Optimization through AFM Data

To illustrate the technique, Dr. Atthi presented a demonstration study on silicon trench structures (SiC wafers being more difficult to procure). The trenches, 2 µm wide of line-and-space (L/S) pattern and 2 µm depth, were fabricated with oxide hard masks and deep reactive ion etching (DRIE). Post-etch, a series of process steps were applied to smooth sidewalls:

1. **Wet oxidation** at 900°C for 40 minutes in forming gas ambient.
2. **Oxide etch-back** to remove oxidized roughness peaks.
3. **High-temperature annealing** for silicon flattening surface in nitrogen at varying temperatures (800°C, 900°C, 1000°C).
4. **Additional thin oxide deposition** for further smoothing on one sample.

Five samples were prepared with different annealing conditions. Using the NX-3DM, five points across each 6-inch wafer were measured automatically according to a predefined recipe.

The results showed clear trends:

- **Pre-flattening sample:** Sidewall roughness higher, bottom roughness elevated.
- **Annealed at 800°C:** Significant reduction in both sidewall and bottom roughness without changing trench dimensions.
- **Higher annealing temperatures:** Further smoothing, but diminishing returns.
- **Oxide re-deposition:** Additional improvement in smoothness.

In the optimized condition, sidewall roughness was reduced to ~1 nm (left) and 2.2 nm (right), while preserving trench geometry—critical for electrical performance.

Comparison with Other Techniques

In his talk, Dr. Atthi compared 3D-AFM to other CD and profile measurement methods:

- **Critical Dimension-Scanning Electron Microscope (CD-SEM):** Good for top-down CD measurement but limited in capturing full sidewall profile and roughness.
- **Optical profilers (OP) and white-light interferometer (WLI):** Non-contact and fast, but limited by optical resolution and unsuitable for deep, narrow trenches.
- **Cross-sectional SEM (X-SEM) and Focused ion beam (FIB):** Provides profile detail, but destructive and low-throughput.
- **Conventional AFM:** High resolution for surface roughness, but cannot access sidewalls.

The 3D-AFM offers a **non-destructive, high-resolution, full-profile measurement**—with automation making it suitable for in-line process control as the comparison shown in **Table 1**.

	3D-AFM (NX-3DM)	AFM	OM, OP, WLI	CD-SEM	X-SEM
Non-destructive	☺	☺	☺	☺	
Pattern height, depth	☺	☺	☺		☺
Pattern width (CD, Line-and-space)	☺		☺	☺	☺
Sidewall angle (SWA)	☺		☺		☺
Sidewall profile (corner shape)	☺		☺		☺
Sidewall roughness	☺				
Line-edge roughness (LER) and line-width roughness (LWR)	☺	☺		☺	
Surface roughness	☺			☺	
Long axis profile (Length)	☺				

Table 1. *Advantages of 3D-AFM to measure the trench etched profile compared to other conventional methods.*

Implications for SiC Power Device Manufacturing

The implications for SiC power devices are direct. As Dr. Atthi noted, trench geometry and surface finish are not cosmetic details—they are central to device operation:

- **Sharp bottom corners** concentrate electric fields, leading to premature breakdown.
- **Rough sidewalls** create leakage pathways that reduce efficiency and reliability.
- **Dimensional variation** across wafers can lead to performance spread and yield loss.

By providing detailed, repeatable 3D data on trench structure, automated AFM enables fabs to tune etch and smoothing processes, validate process stability, and catch deviations before they impact production.

Conclusion: Automation Meets Nanoscale Insight

The combination of wide bandgap semiconductors like SiC and advanced trench architectures is reshaping power electronics. But these innovations place unprecedented demands on process control.

Automated 3D-AFM, as demonstrated by Dr. Atthi, offers the precision, repeatability, and throughput needed to meet these demands. By measuring critical dimensions, sidewall roughness, and trench profiles at sub-nanometer precision—non-destructively and across entire wafers—AFM becomes not just a characterization tool, but a process enabler.

As Dr. Atthi concluded, "The fully automated 3D-AFM from Park Systems provides reliable, repeatable, and high-quality data that directly supports the performance and reliability of next-generation power devices."

References

1. J. Wei, et al., "Review on the Reliability Mechanisms of SiC Power MOSFETs: A Comparison Between Planar-Gate and Trench-Gate Structures," IEEE Transactions on Power Electronics, 38, 7, pp. 8990-9005, (2023), DOI: 10.1109/TPEL.2023.3265864
2. Yoo, SB., Yun, SH., Jo, AJ. et al., "Automated measurement and analysis of sidewall roughness using three-dimensional atomic force microscopy, " Appl. Microsc. 52, 1 (2022). https://doi.org/10.1186/s42649-022-00070-5
3. https://www.rohm.com/news-detail?news-title=new-4th-gen-sic-mosfets&defaultGroupId=false

About Dr. Nithi Atthi

Dr. Nithi Atthi is the Fab Manager at the Thai Microelectronics Center (TMEC), part of Thailand's National Electronics and Computer Technology Center (NECTEC). He holds degrees in Materials Engineering and Engineering Management from Kasetsart University and earned his M.S. and Ph.D. in Electronics and Applied Physics from the Tokyo Institute of Technology under the MEXT Monbukagakusho scholarship. Dr. Atthi is a recipient of several international fellowships, including Green Talent (Germany), HOPE Meeting (Japan), STS Forum Young Leader (Japan), and the UK's Leaders in Innovation Fellowship. He has authored over 45 journal publications, delivered 122+ academic talks, and holds 27 patents. His research spans wafer fab design, semiconductor process integration (FinFETs, GAA-FETs, MEMS), advanced lithography, and functional surfaces.

Dr. Nithi Atthi

NanoScientific Editor's Supplement

Why 3D-AFM is Key for Next-Generation SiC Power Devices

The Device Shift Driving New Metrology Needs

Silicon carbide (SiC) has rapidly become the material of choice for high-voltage, high-efficiency power devices used in electric vehicles, renewable energy, and industrial systems. Unlike traditional planar silicon devices, modern SiC MOSFETs use **deep trench structures** to achieve lower resistance and higher voltage handling.

But these trenches introduce a new problem: **every micron of their geometry can make or break device performance.** A sharp corner can create a breakdown point; a slightly rough sidewall can increase leakage. That means **measuring the shape and smoothness of each trench has become a critical part of manufacturing**.

The Metrology Challenge: Seeing Inside the Trench

Traditional inspection tools are limited:

- **SEM** can image trench profiles but is destructive for cross-sections.
- **Optical methods** lack the resolution for nanoscale sidewall detail.
- **Conventional AFM** measures flat surfaces well, but can't capture vertical walls.

To truly understand a trench, we need **all dimensions—top, bottom, sidewalls—measured at nanometer precision, and without destroying the sample.**

This is where **3D-AFM** enters the picture.

3D-AFM: Complete, Non-Destructive Profiles

Unlike conventional AFM, automated 3D-AFM systems tilt the scanning head to access trench sidewalls. By combining measurements from **multiple angles**, they build a **full 3D map of the trench**, including:

- **Critical Dimensions (CD)** at top, middle, and bottom
- **Sidewall slope** and uniformity
- **Corner curvature** at trench base
- **Sidewall roughness** in smooth, measurable detail

All of this is done **non-destructively** and can be repeated across wafers for process control.

From Lab Instrument to Production Tool

What makes 3D-AFM transformative is its move from research labs into semiconductor fabs. Automated systems now handle:

- **Full wafer sizes (6–12 inches)**
- **Robotic loading (SMIF/FOUP)**
- **Recipe-driven measurements** for repeatable results
- **Automated tip exchange** for continuous operation

This automation means 3D-AFM can be a **routine in-line tool**, not just a specialized characterization method.

Why This Matters for SiC Devices

In SiC trench MOSFETs, **geometry is directly linked to performance**. A smoother trench bottom reduces electric field stress; uniform sidewalls lower leakage risk; consistent CDs ensure predictable switching.

3D-AFM delivers the **data fabs need to keep these parameters under control**, helping devices reach their intended performance and reliability targets.

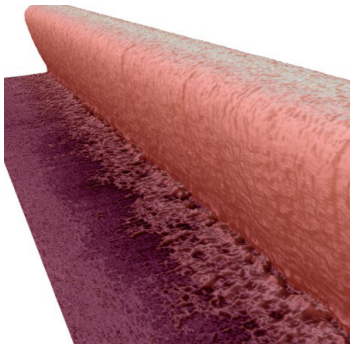

Fig. 1. 3D-AFM image of a photoresist line pattern

High-resolution sidewall and surface characterization of a photoresist pattern, captured using Park NX-3DM. The image reveals detailed roughness critical for evaluating lithography quality and CD uniformity.

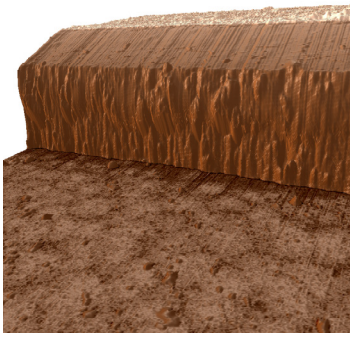

Fig. 2. 3D-AFM image of a semiconductor sidewall

High-resolution 3D topography of a semiconductor structure showing vertical sidewall roughness. Captured using Park NX-3DM with tilted scanning, this image enables critical sidewall analysis essential for process optimization in advanced semiconductor manufacturing.

PROBING SURFACES IN REALISTIC CONDITIONS: AFM IN CONTROLLED ATMOSPHERIC ENVIRONMENTS

Dr. Patrik Schmutz, Empa – Swiss Federal Laboratories for Materials Science and Technology
Adapted from Presentation, Edited by NanoScientific

Introduction: AFM at the Interface of Reality and Control

At the 2024 NanoScientific Forum Europe, Dr. Patrik Schmutz brought the audience into the intricate world of surfaces as they exist in real environments—not just in the clean confines of a laboratory. His research at Empa focuses on the electrochemical processes and surface reactivity of metals and alloys under conditions that mimic industrial and environmental realities.

Atomic Force Microscopy (AFM) is already renowned for its ability to probe nanoscale topography and material properties. But for corrosion science, surface functionalization, and interface chemistry, the challenge lies in reproducing the environment in which a material truly operates—where humidity, temperature, and contaminants interact in complex ways.

Dr. Schmutz's group has taken AFM into this space by modifying instruments to operate under precisely controlled atmospheric conditions. These environmental AFM experiments allow the direct study of solid–liquid interfaces—even when the "liquid" exists as a monolayer of adsorbed water or a thin electrolyte film—and the electrochemical processes that arise.

The result is a unique capability: nanoscale electrochemical reactivity measured in a realistic, tunable environment, directly linked to material performance in service.

From Lab to Field: Why Environment Matters ?

In industrial and natural environments, materials rarely encounter perfectly dry or perfectly wet conditions. Instead, they operate in fluctuating humidity, exposed to aggressive ions, pollutants, and temperature cycles. Even a single monolayer of adsorbed water can generate a solid-liquid interface and profoundly alter electrochemical potentials, adhesion, wettability, and surface energy.

"AFM is not just a topography tool," Dr. Schmutz reminded the audience. "It can track electrical, magnetic, mechanical, and wetting properties—but these are strongly environment-dependent. To study them realistically, we need environmental control."

His group works extensively with electrochemical processes at metallic surfaces, including oxidation, corrosion, and functionalization of reactive as well as medical-grade alloys. Over the years, they have adapted commercial AFMs to make use of small, sealable environmental chambers capable of regulating humidity, temperature, inert gas atmosphere, and even dosing with reactive gases or ions.

These modifications make it possible to bridge the gap between macroscopic electrochemical measurements (such as impedance spectroscopy) in bulk electrolytes and nanoscale phenomena at the solid–liquid interface.

Measuring Surface Potential in a Thin Water Layer

One focal point of Dr. Schmutz's presentation was surface potential mapping using Scanning Kelvin Probe Force Microscopy (SKPFM) often referred to simply as KPFM in the AFM community—under controlled atmospheric conditions.

At the heart of this approach is the recognition that the first few molecular layers of water on a metal surface define much of its electrochemical behavior (Fig. 1A). Even at moderate humidity, a stable water monolayer forms, with a steep potential gradient across the Helmholtz plane.

In the presence of liquid layers, KPFM can detect these potential differences best by lifting a conductive AFM tip above the surface—avoiding direct disturbance of the delicate water layer—and applying a bias to nullify the electrostatic forces. When such a nm-thick solid-liquid interface is formed by a controlled exposure to humidity/water, it can be demonstrated that the potential measured (referred to Volta potential) on pure metals correlate linearly with the Open Circuit Potentials (OCP) obtained versus a well-defined Hg/HgCl Calomel electrode (SCE) in bulk water. The measured potential contains, in both cases (KPFM and bulk), a significant charge contribution from the nm-thick passive oxides, Fig. 1A.

For thicker oxides, space charge effects then become a significant contribution to the solid-liquid interface potential gradients. Fig. 1B presents the example of two trends in thick (see cross-section after 100V anodizing) anodically grown amorphous barrier oxides displaying various space-charge contributions. KPFM allowed us to investigate the charge building up as a function of oxide defect densities. In the presented example, KPFM characterization identified a remarkable difference in the potential evolution for oxides grown on 99.99% and 99.5% pure aluminum. The very high potentials measured for the 99.5% Al are attributed to denser oxide with less defect migration ability during the high field growth anodizing process compared to the lower density oxides formed on 99.99% Al [3]. This "density" difference has been cross-validated by other characterizations [3].

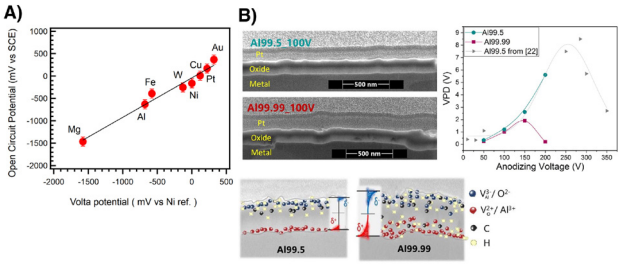

Fig. 1. *Potential establishing on the surface is closely related to the charge distribution across the solid-liquid interface.* A) *Electrochemical potential scale" (also denominated as Volta potential) determined with the KPFM methods and compared the classically determined OCP in solution (versus Ag/AgCl reference electrode)[1,2].* B) *For thicker anodized oxides [3]: Cross section, related KPFM characterization indicating that the oxide space charge is one key contribution to the solid-liquid interface potential, sketched in-depth distribution of charges for different oxide densities*

This detailed analysis of the different contributions in the solid-liquid interface potential gradients can obviously be best used with the environmental AFM /KPFM combination on micro and nanosized heterogeneous materials or components. For multiphase alloys, such as aluminum alloys with intermetallic particles (see SEM characterization in Fig. 2A), this potential mapping reveals nanoscale galvanic coupling: magnesium-rich particles appear at low potential (anodic sites), while copper- or iron-rich intermetallics appear at high potential (cathodic sites). Being able to evidence these different "surface reactivities" is essential for predicting corrosion.

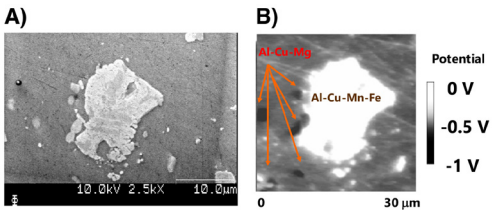

Fig. 2. *Laterally resolved surface reactivity assessment on Aluminum AA2024T3 alloy with local microgalvanic effect between intermetallics and the Al matrix investigated:* A) *SEM image of an aluminum alloy microstructure,* B) *KPFM potential mapping of the same microstructure.*

Environmental Transitions: Dry, Humid, and Wet Regimes

The previously presented examples obviously already require well defined environmental control. Going one step further in the understanding of surface reactivity and degradation mechanism can be achieved by systematically varying humidity. Dr. Schmutz's group has shown how the electrochemical behavior of multiphase materials changes across three environmental regimes:

- **Dry regime (below ~20% RH):** Surfaces are covered only with oxygen and oxide layers. KPFM shows strong potential contrast between phases, but the absolute potentials carry little electrochemical meaning.
- **Humid regime (20–70% RH):** A monolayer of water forms, enabling a solid-liquid interface with a Helmholtz-like charge gradient to build up. Potential values drop toward relevant electrochemical equilibrium, but galvanic interactions between phases are still not active evidenced by the fact that potential contrasts are still present between phases.
- **Wet regime (>70% RH):** A thicker continuous electrolyte layer forms. Potentials across the surface homogenize as galvanic coupling equilibrates the system. In many materials, this transition from humid to wet conditions marks the onset of aggressive corrosion. This humidity threshold is, for example, very critical for electronic micro and nanodevices.

To highlight this analysis, one striking example is represented by tungsten carbide–cobalt hardmetals composites (**Fig. 3**)used, for example, in cutting tools and drill bits. While tungsten carbide is chemically stable in neutral environments, cobalt binder phases are highly reactive already in neutral water and slightly acidic conditions (**Fig. 3D**). In dry conditions (**Fig. 3A**), and as mentioned previously, oxidation takes places, but no solid-liquid interfaces are formed and the high measured potentials for Co (dark areas) and WC (bright areas) are not representative of electrochemical conditions. At intermediate humidity (**Fig. 3B**), cobalt becomes electrochemically active, the KPFM measurements indicates around -0.4 V close to the thermodynamic redox potential for the Co^{2+}-Co equilibria as shown on the Pourbaix diagram (**Fig. 3D**). In wet conditions (**Fig. 3C**: 90% RH)Co is dissolving rapidly driven by galvanic coupling as indicated by the uniform and low potential (Co Redox potential) measured by KPFM and aggravated by the larger surface area of the carbide grains—degrading the material's mechanical integrity.

This evolution and the related surface reaction mechanisms are then summarized in **Fig. 4**. The initially very large potential difference measured upon dry oxidation (4% RH), experiences first a shift toward more negative "electrochemically" relevant potentials in humid environments (65%) before a complete homogenizing and galvanic coupling is taking place in wet environments (90% RH). Dissolved ions contribute to a strengthening of this coupling effect by increasing the ionic conductivity and the nm-thick water layer.

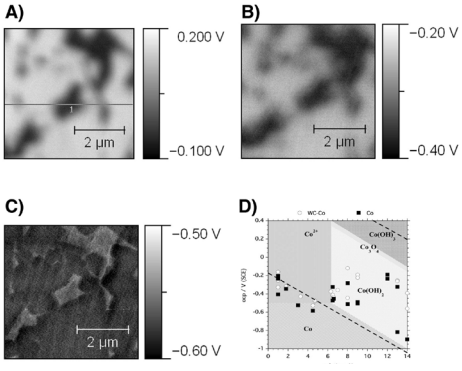

Fig. 3. *Relative humidity (RH) dependent KPFM potential information obtained on the same composite microstructure:* A) *in dry environment (4% RH),* B) *humid environment (65%) and* C) *wet environment (90%);* D) *Co Pourbaix diagram displaying the thermodynamically expected potentials and passive oxide/hydroxide stability domains [4]. The black squares and open dots are experimentally measured macroscopic OCP for Co and WC-CO as function of the electrolyte pH*

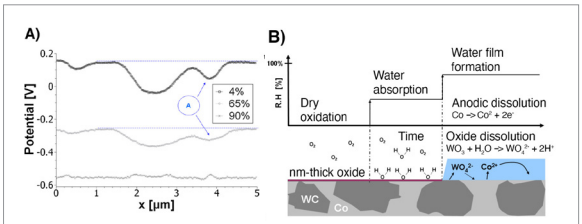

Fig. 4. *Mechanistic explanation of the observed phenomenon during environmental KPFM characterization:* A) *Evolution of the potential profile (for location, see line 1 on* Fig. 3A) *on the Co and WC phases,* B) *sketched description of the water (immobile versus mobile) building up and influence of ionic mobility on the galvanic coupling.*

Coupling AFM with Local Electrochemical Probes

While KPFM reveals potential distributions, it does not provide direct kinetic data. For this, Dr. Schmutz's group employs complementary techniques such as **Electrochemical nanocapillary methods**—a point-by-point method in which a nanocapillary containing electrolyte is positioned on the surface (**Fig. 5A**).

By polarizing individual phases separately, this capillary-based method can measure local anodic and cathodic currents, revealing why certain phases corrode faster than others. Following on the experiments presented in **Fig. 3**, the electrochemical polarization curves performed with a 300 nm diameter capillary on the Co and WC phases (**Fig. 5B**) confirmed that, cobalt in hardmetals exhibits high anodic dissolution currents, while tungsten carbide shows low cathodic current density. Two measurements for different Co areas are displayed for the slightly acidic electrolyte (0.1M KH_2PO_4) used (**Fig. 5C**): one showing very high activation currents and the other one with very low passive currents. These two very different behaviors are however expected given the fact that cobalt lies in this electrolyte at its stability boundary (see Pourbaix diagram, **Fig. 3D**). The extremely important information obtained in **Fig. 5C** by this additional characterization is:

- First in the electrochemical potential measurements. The values of around -0.2V for WC and -0.4V for Co are totally in line with the KPFM characterization in humid environment.
- The reaction kinetics indicate that the anodic dissolution of Co is much faster compared to the cathodic reduction on WC—confirming the non-polarizable, sacrificial role of cobalt in galvanic coupling justifying that the whole surface is polarized to its low potential.

This local kinetic information obtained by the nanocapillary technique is essential for understanding how isolated defects or inclusions can dictate the corrosion behavior of an entire component, but the KPFM analysis was in fact sufficient to document the surface reactivity mechanisms and the non-polarizable nature of the Co areas!

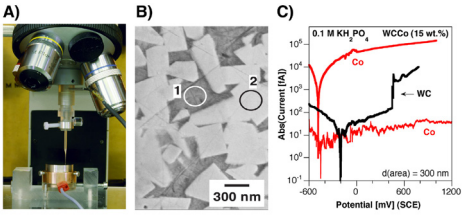

Fig. 5. *Locally measured reaction kinetic with electrochemical nanocapillary measurements:* A) *picture of the setup;* B) *measured areas;* C) *polarization curves obtained from the different single phases.*

Industrial Case Study: Blistering of Aluminum-Tin-Coated Bearings

The power of environmental AFM becomes clear in industrial case studies. Dr. Schmutz presented the example of large bearings with a Al-Sn top layer over a nickel interlayer and bronze substrate, **Fig. 6A**. The tin layer acts as a solid lubricant, reducing friction in service. However, in certain polluted climates, bearings developed surface blisters after only a year in storage. Cross-sectional analysis revealed localized delamination, typically around 100 µm and corrosion beneath the coating, **Fig. 6B**.

Environmental AFM measurements of fresh coatings cross-section showed that under high humidity (90% RH), tins rapidly oxidize and migrate away from the interface. When sulfur-containing pollutants were additionally introduced, the oxidation products became voluminous, causing mechanical disruption of the coating. KPFM maps showed localized high-potential regions adjacent to reactive dissolving zones—conditions ideal for galvanic corrosion. The degradation rate measured in the laboratory under environmental control—about 150 nm (**Fig. 6D**) trenching at the interface (**Fig. 6C**) after 18 hours of aggressive environment exposure, might not seem a lot but—closely matched the field-observed blister growth rate of 70 µm/year. The conclusion was clear: failure could only be reproduced in this environment and required the combined effect of high humidity and sulfur pollution, conditions common in industrial polluted environments.

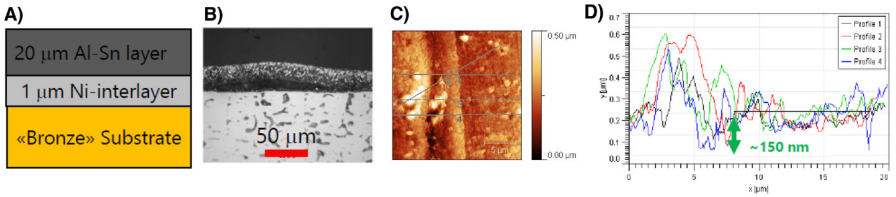

Fig. 6. *Aluminum – Tin coating on Brass substrate degradation:* A) *schematic material description;* B) *Cross-section of blistered (around 100 µm in size) coating after 1 year of industrial atmosphere exposure;* C) *AFM topography measured in cross section after 18 hours exposure in sulfur containing 90% RH environment;* D) *linescans showing around 150 nm trenches at the coating substrate interface where blistering subsequently occurred.*

Conclusion: AFM as a Window into Real-World Interfaces

Through carefully controlled atmospheric experiments, Dr. Schmutz's group has shown that AFM can go far beyond imaging. By combining topography, potential mapping, and local electrochemistry under realistic environmental conditions, AFM becomes a predictive tool for material performance.

Key takeaways from his work:

- Realistic surface reactivity and electrochemical behavior emerges only when a solid–liquid interface exists—even as a thin adsorbed film.
- Surface potential mapping correlates closely with macroscopic corrosion tendencies if environmental conditions are well defined during the AFM characterization.
- Transitions between dry, humid, and wet regimes are critical thresholds for corrosion initiation of heterogeneous materials and components
- Industrial failures often involve environmental synergies, such as humidity plus pollutants, which can be reproduced and quantified in controlled closed chambers in the laboratory.

As Dr. Schmutz summarized for the NSFE audience, "An AFM with environmental control lets us look at surfaces the way they live in the real world." This approach is proving indispensable for industries where durability, corrosion resistance, and functional coatings determine long-term performance.

About Dr. Patrik Schmutz

Dr. Patrik Schmutz is a leading researcher and Group Leader in the Joining Technologies & Corrosion laboratory at Empa (empa.ch)—the Swiss Federal Laboratories for Materials Science and Technology—located in Dübendorf, Switzerland. He also holds a lecturer position in Materials Science at ETH Zürich (ch.linkedin.com).He obtained his PhD degree from EPF Lausanne, Swizerland followed by post-doctoral research stays at Ohio State University and ETHZ.

Dr. Schmutz leads research on electrochemical oxidation/passivation and medical implant surfaces, focusing on the reactivity and stability of functionalized surfaces in real-world environments—from humid, polluted atmospheres to complex biological media. His group employs a broad suite of techniques, including environmental AFM (notably SKPFM), local electrochemical methods, impedance spectroscopy, electrochemical quartz microgravimetry, HAXPES/XPS, and spectroscopic imaging, to interrogate processes like passivation, galvanic coupling, and corrosion kinetics in advanced materials and biomedical implants. His work spans both fundamental understanding and applied solutions in industries ranging from microelectronics and aerospace to civil engineering and healthcare.

For more information, contact patrik.schmutz@empa.ch or look at Empa - Joining Technologies and Corrosion - Surface Electrochemistry.

Dr. Patrik Schmutz

References

1. P. Schmutz, G.S. Frankel, "Characterization of AA2024-T3 by Scanning Kelvin Probe Force Microscopy", *Journal of the Electrochemical Society, 145(7), 2285-2295(1998)*
2. V. Guillaumin, P. Schmutz, G.S Frankel, "Characterization of Corrosion Interface by the Scanning Kelvin Probe Force Microscopy Technique", *Journal of the Electrochemical Society, 148(5), B163-173 (2001)*
3. M. Gonźalez-Castãno, M. Döbeli, V.Araullo- Peters, L.P.H. Jeurgens, P. Schmutz, C. Cancellieri "Substrate purity effect on the defect formation and properties of amorphous anodic barrier Al_2O_3" *Journal of the Electrochemical Society, 165(7), C422-C431 (2018)*
4. F. Evangelisti, M. Stiefel, O. Guseva, R. Partovi Nia, R. Hauert, E. Hack, L.P.H. Jeurgens, P. Schmutz, C. Cancellieri, "Electronic and structural characterization of barrier-type amorphous aluminium oxide", Electrochimica Acta, 224, 503-516 (2017)
5. S. Hochstrasser(-Kurz), C. Latkoczy, D. Günther, S. Virtanen, P.J. Uggowitzer, P. Schmutz "ICP-MS, SKPFM, XPS and microcapillary investigation of the local corrosion mechanisms of WC-Co hardmetal" *Journal of the Electrochemical Society, 155(8), C415-C426 (2008)*

NANOPATTERNING ON 2D MATERIALS: A CASE STUDY ON GRAPHENE BY AFM-BASED NANOLITHOGRAPHY

Dr. Jake Kim and Dr. Rocky Nguyen, Park Systems Corp.

Introduction

Graphene, a single layer of carbon atoms arranged in a two-dimensional lattice, has attracted significant attention due to its exceptional electrical, thermal, and mechanical properties[1-3]. Its potential applications range from nanoelectronics to sensors, catalysis, and energy storage. However, precise manipulation and patterning of graphene at the nanoscale remain challenging, hindering the utilization of its unique characteristics in practical applications. Atomic Force Microscopy (AFM)-based nanolithography has emerged as an effective method for nanoscale fabrication[4,5]. AFM-based nanolithography enables the direct writing of patterns on a material's surface with nanometer precision. This technique employs a sharp AFM tip to induce local modifications to the material, facilitating the creation of intricate patterns on graphene layers[6] (**Fig. 1**). The cutting process involves a careful balance of various parameters, including tip bias, AFM tip applied force and approach speed, and environment conditions, to achieve optimal results. Optimization of these parameters is essential for effectively cutting graphene and generating well-defined nanopatterns.

In this study, we conducted a feasibility test to optimize AFM-based nanolithography parameters to achieve precise nanopatterning on a single layer of graphene (**Fig. 2**). Through a series of trials, we systematically investigated the influence of key variables on the cutting quality and resolution of nanometer-scale lines. By enhancing the understanding of AFM-based nanolithography techniques, we aim to contribute to the advancement of graphene applications across various fields, particularly in the development of next-generation nanodevices.

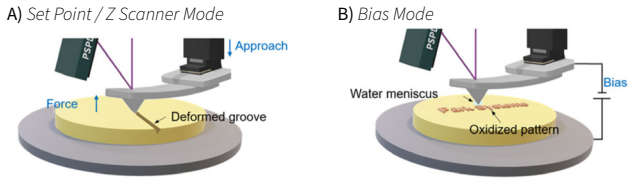

Fig. 1. *AFM-based nanolithography.* **A)** *Set Point / Z Scanner Mode: the AFM system exerts a significant force to mechanically deform the sample surface by scratching it.* **B)** *Bias Mode: AFM tip bias is applied on the patterned area to create an oxidation layer (height approx. 1-2 nm) on a bare surface.*

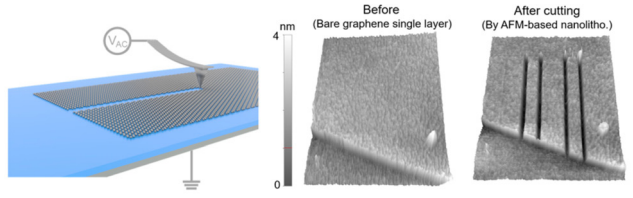

Fig. 2. *Cutting thin layer graphene by AFM-based nanolithography.*

Materials and Methods

Thin graphene layers on a silicon (Si) wafer were prepared to evaluate the cutting or patterning of graphene layer by AFM-based nanolithography.

For AFM-based nanolithography, a commercial AFM system, Park NX10 (Park Systems), was used[7]. The AFM system and probe were calibrated prior to experiments to ensure accuracy. The two detailed modes of AFM-based nanolithography used in this study are described as follows.

1. **Set Point / Z Scanner Mode (Mechanical method):** In mechanical AFM lithography, the AFM tip applies a controlled, high force to physically etch or "cut" through the graphene layer. By tracing a predefined pattern, the tip can cut specific shapes or pathways into the graphene with nanometer precision.
2. **Bias Mode (Electrochemical method):** In this mode, a bias voltage is applied between the AFM tip and the substrate, creating an electric field that induces a local oxidation reaction at the graphene surface. This results in oxidized graphene regions that can be selectively removed, effectively "cutting" the graphene. It is especially useful for precise and controlled modifications of graphene without requiring high physical force.

Investigation of graphene cutting quality under varying parameters

The mechanical cutting method in AFM-based nanolithography is straightforward[8]. It cuts the graphene layer by precisely controlling the force applied to it and can be performed under ambient conditions, making it more accessible than methods requiring vacuum or controlled environments. However, this method has some notable drawbacks. The AFM tip is prone to wear and damage due to high force applied during cutting, which can reduce accuracy over time and necessitate more frequent tip replacements. As shown in **Fig. 3**, there is also a risk of unintended damage or deformation to the surrounding graphene due to the mechanical force, which can degrade the quality of the patterned structure. This often results in rough or jagged edges along the cut regions—especially at higher forces—potentially impacting the electronic properties of graphene where smooth edges are essential.

An alternative method, Bias Mode in AFM-based nanolithography, was also tested with various parameters. This method involves a bias voltage between the AFM tip and the substrate generates a localized electric field at the contact point or near-contact region with the graphene. This electric field causes water molecules from the ambient environment or intentionally introduced moisture to undergo electrolysis, producing reactive oxygen species like hydroxyl ions. These reactive oxygen species interact with the carbon atoms in graphene, leading to oxidation and transforming specific portions into graphene oxide, which has distinct electrical and chemical properties from pristine graphene. The use of AC bias enhances this process by generating a periodically oscillating electric field, which prevents continuous charge buildup and reduces unwanted side reactions. This field enhances the formation of reactive oxygen species, enabling precise, localized cuts[9,10].

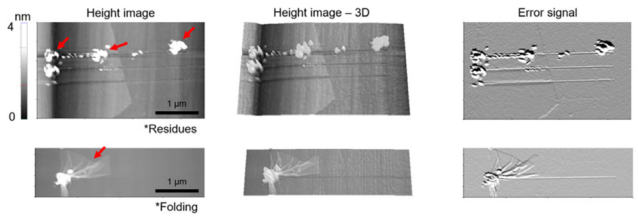

Fig. 3. *Mechanical cutting of graphene using AFM-based nanolithography in Set Point Mode. Lines are formed by applying force after tip-surface contact, inducing surface scratches.*

We first demonstrated graphene cutting possibilities according to the applied bias. Consequently, the applied voltage significantly affected the extent and depth of the oxidation on graphene, which influences the degree of cutting (**Fig. 4**).

1. **No bias (0V)**: At low or zero voltage, oxidation is negligible due to an insufficient electric field to initiate the electrolysis of water molecules and generate reactive oxygen species. As a result, no significant cutting or oxidation occurs on the graphene surface.
2. **Low bias (3V):** With moderate voltage, a controlled oxidation process begins. At this range, the electric field is sufficient to start generating reactive oxygen species, which then interact with the graphene surface to create shallow, localized oxidized regions. These regions are often less deep and don't fully "cut" through the graphene, making them more suitable for modifying surface properties or creating conductive paths without fully isolating sections of graphene.
3. **High Bias (10V):** At higher voltages, the oxidation process intensifies as the stronger electric field generates more reactive oxygen species and increases the rate of oxidation. This can lead to deeper oxidation that might extend through the graphene layer, effectively "cutting" or isolating parts of it. At sufficiently high voltages, oxidation depth can be controlled to fully penetrate the graphene layer, creating distinct regions that are electrically separated from each other.

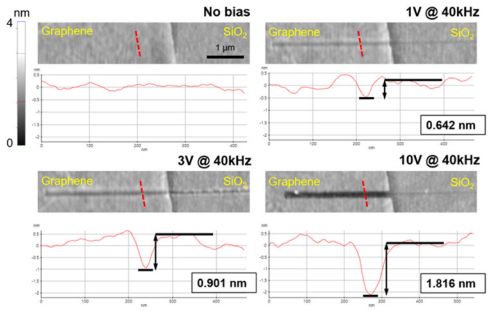

Fig. 4. *Electrically graphene cutting by AFM-based nanolithography with AC bias mode. At 1 and 3 V, the lines are thin and blurry; however, when 10 V is applied, the etching line is successfully formed with smooth edges and no residue.*

Humidity is one of the most important factors for the success rate of graphene cutting via AFM-based nanolithography. The presence of ambient water molecules is critical, as they enable the generation of reactive oxygen species needed for oxidation[11]. In **Fig. 5**, at 10% relative humidity, the water layer between graphene and the Si substrate is minimal or nearly absent, which limits reactive oxygen species production and leads to a very low success rate for cutting. Oxidation under these conditions is weak or incomplete, resulting in inconsistent outcomes. When humidity increases to 20–40%, the water layer is slightly thicker, providing more reactive oxygen species; however, the amount remains insufficient for deep or reliable oxidation, producing shallow or incomplete cuts and only a slight improvement in success rate.

At humidity levels above 60%, the water layer is well-established, offering ample water molecules for reactive oxygen species production. This level is confirmed to be optimal for the Bias mode of AFM-based nanolithography, as it enables a strong, stable oxidation reaction that results in deep, consistent cuts with high success and precision[9].

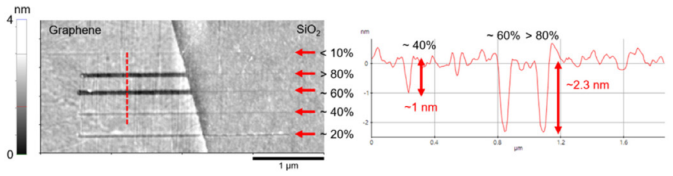

Fig. 5. *Graphene cutting quality according to humidity environment. A humid environment of 60% or more is recommended for accurate cutting.*

The presence of a water layer between the graphene and the Si substrate can also influence the result in graphene cutting by AFM-based nanolithography. This water layer, which is present due to ambient humidity or adsorbed water molecules, plays an essential role in the anodic oxidation reaction by providing a medium for electrochemical processes. **Fig. 5** shows that water molecules are necessary to produce reactive oxygen species through electrolysis. The water layer between the graphene and the Si substrate can contribute additional water molecules, enhancing the local availability of reactive oxygen species at the oxidation site[9].

Based on this theory, it is hypothesized that, given adequate time for a water bridge to form between the AFM tip and the sample surface, the directional dependence of the cutting process can be mitigated. Here, "adequate time" does not refer merely to a slow scan speed; rather, it involves a deliberate deceleration of the AFM tip immediately prior to contact with the sample, allowing sufficient time for the water bridge to establish itself between the AFM tip and the sample surface. As shown in **Fig. 6**, when the AFM tip was allowed to contact the sample (graphene or Si substrate) very slowly, it was confirmed that the graphene was successfully cut in any direction. This is because when the AFM tip is very close to the graphene surface, a water bridge forms first, causing local oxidation and removing the graphene beneath it. SmartScanTM (Park Systems' AFM operation software) enables precise control of these parameters, resulting in more consistent and effective graphene cutting.

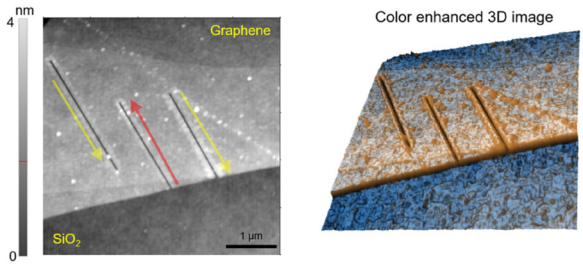

Fig. 6. *Cutting direction analysis with AFM tip approach speed. When the approach speed is sufficiently slow, the cutting direction does not need to be considered.*

In conclusion, our findings show that graphene cutting using the Bias mode of AFM-based nanolithography can be effectively achieved when the AFM tip approaches the sample surface very slowly, allowing adequate time for a water bridge to form between the tip and the surface, with a bias of 3 V or higher, and under a humidity level of 60% or more. This method is effective for both simple line patterns and more complex geometries, as demonstrated in **Fig. 7**.

Continued on page 10

CHARGE-TRANSFER POLARITONS IN VAN DER WAALS HETEROJUNCTIONS: UNLOCKING NEW FRONTIERS IN GRAPHENE PLASMONICS

Prof. Brian Kim, University of Arizona
Adapted from Presentation, Edited by NanoScientific

Introduction: Expanding the Design Space of 2D Polaritons

At the 2024 NanoScientific Symposium, Prof. Brian Kim from the University of Arizona introduced a major step forward in nanophotonics—the creation of highly tunable charge-transfer polaritons in van der Waals (vdW) heterojunctions. His work demonstrates how precisely engineered oxide–graphene interfaces can generate stable, low-loss graphene plasmons with exceptional lateral doping resolution, all without the drawbacks of traditional gating or lithography.

Polaritons—quasiparticles formed from the strong coupling of light and matter—are a foundation for advanced optical and quantum devices. In graphene, surface plasmon polaritons (SPPs) combine extraordinary confinement (more than 100× shorter wavelength than light in vacuum) with low intrinsic loss, tunability, and compatibility with layered materials. However, their implementation has been hindered by a practical challenge: how to introduce large carrier densities into graphene with nanometer precision, without physically degrading the lattice or blurring the doping profile.

Prof. Kim's solution uses a subtle but powerful physical effect—work function mismatch at engineered oxide interfaces—to "write" doping patterns directly into pristine graphene.

Polaritons in 2D Materials: Why Graphene Is Special

In polaritonic systems, electromagnetic waves couple strongly with excitations such as plasmons (collective oscillations of electrons) or phonons (lattice vibrations). At the interface between two materials with opposite signs of dielectric function, these hybrid modes can propagate along the boundary.

Graphene is an ideal host for polaritons because:

- SPPs exist only at high doping levels, enabling tunable activation by carrier density.
- Plasmonic modes in graphene are low-loss due to Pauli blocking of electron–hole scattering, unlike metals where damping from conduction electrons is unavoidable.
- Its vdW nature allows precise stacking with other 2D materials to hybridize modes and engineer novel dispersion relations.

Moreover, graphene's plasmons produce strong confinement and enable manipulation of optical modes deep below the diffraction limit—over a broadband from THz into the mid-infrared regime.

The Challenge: Patterning Graphene Plasmonic Cavities Without Detriment

To take advantage of these properties, one must be able to create nanoscale patterns of high carrier density to realize plasmonic cavities or photonic crystals while preserving the exceptional mobility and crystalline perfection of graphene.

Traditional strategies—such as directly etching graphene into nanostructures or patterning local gates beneath it—come with serious drawbacks. Etching produces rough edges that scatter plasmons. Patterned gates limit flexibility, introduce dielectric inhomogeneities, and require close spacing that constrains optical mode design. Both approaches blur the lateral doping profile, reducing mode sharpness and cavity Q factors.

Prof. Kim's group sought an alternative that could:

- Avoid physical damage to the graphene lattice.
- Precisely control doping strength and profile shape.
- Eliminate the need for patterned gates.

Work Function Mismatch: Gate-Free Ambipolar Doping

The breakthrough comes from harnessing electrostatics. When two materials with different work functions are brought into intimate contact, charge-transfers across the interface until the Fermi levels align.

Prof. Kim's team transfers atomically thin layers of high–work function transition metal oxides on graphene. In their work, tungsten oxide (WO_x) is created in situ by oxidizing tungsten diselenide (WSe_2) layers using ultraviolet ozone treatment. Crucially, this oxidation is *self-limiting*: only the outermost monolayer of WSe_2 converts to WO_x, while the underlying structure remains intact.

This approach offers several advantages:

- No etching or gate electrodes are required.
- The oxide induces substantial, uniform hole doping through work function mismatch.
- Lateral doping boundaries are atomically sharp.

By designing vdW heterostructures where a high-work-function WO_x sits atop monolayer graphene encapsulated in hexagonal boron nitride (hBN), the group achieves extremely high hole densities (on the order of 4×10^{13} cm^{-2}) without external gating. By substituting WO_x with low–work function zirconium oxide (ZrO_x), Prof. Kim's group achieves electron doping of graphene to similarly high densities, confirming the robustness of the charge-transfer technique. This ambipolar charge-transfer doping significantly expands access to optical properties and transport regimes in vdW heterostructures previously unreachable with conventional electrostatics.

Probing the Charge-Transfer Plasmons via s-SNOM Imaging

To verify charge-transfer and map plasmon propagation, the team employs **scattering-type scanning near-field optical microscopy (s-SNOM)**—a technique that combines atomic force microscopy with infrared illumination at the nanoscale.

In Prof. Kim's images, distinct plasmonic interference fringes appear along the oxide–graphene interface. These standing wave patterns are formed by plasmons launched from the s-SNOM tip, reflected at conductivity boundaries, and interfered on their return. The visibility and uniformity of these fringes confirm both effective doping and high material quality. Fitting the fringe decay to a damped oscillator model yields a plasmon quality factor Q of ~16, already approaching the performance of silver films at comparable frequencies.

Because the oxidation process affects only the exposed surface, the team can control charge-transfer with atomic precision by inserting layers of unoxidized WSe_2 as spacers between WO_x and graphene. Each

monolayer acts as a nanometer-scale buffer, modulating the effective work function mismatch and thus the doping level.

Increasing the spacer thickness reduces the plasmon wavelength (corresponding to reduced carrier density) while improving Q due to diminished scattering from charged impurities in the oxide. Remarkably, a single bilayer spacer (~7 Å thick) reduces scattering enough to raise Q to ~30—surpassing noble metals and approaching the intrinsic phonon-limited behavior of graphene plasmons at room temperature.

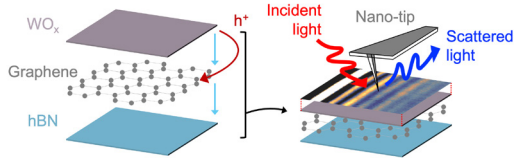

Fig. 1. *Schematic illustration of charge-transfer plasmons in engineered oxide–graphene interfaces imaged via s-SNOM technique.*

Creating Plasmonic Nanocavities Without Physical Etching

This charge-transfer approach enables a powerful fabrication strategy: **mask-defined plasmonic cavities** in continuous graphene. By placing a pre-patterned hBN mask with nanoscale apertures over graphene before oxidation, Prof. Kim's team can locally expose regions to WO_x formation. The result is a pattern of high-density, plasmon-active regions embedded in a continuous sheet of pristine graphene.

s-SNOM imaging confirms strong cavity modes within these regions. Finite-element simulations show that lateral doping transitions sharper than ~6 nm are achieved using this method, yielding well-confined modes without lattice disruption.

The group further demonstrates suspended graphene plasmonic cavities that can be doped from both the top and bottom via WO_x. Dispersion mapping verifies hole-doping, showing that doping density increased by ~30%. Importantly, these suspended cavities support whispering gallery modes, plasmon waves circulating along the cavity perimeter, forming standing wave patterns governed by cavity size and excitation frequency. These modes, observed here in graphene for the first time, demonstrate the potential for control over strong light–matter interactions in engineered 2D cavities.

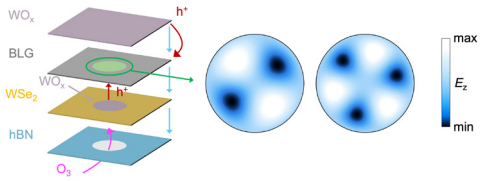

Fig. 2. *Schematic illustration of the realization of plasmonic whispering gallery cavities based on suspended oxide–graphene heterostructures.*

A New Platform for Graphene Plasmonic Nanocavities

Prof. Kim's team demonstrates how the charge-transfer graphene plasmonic nanocavities described above can open up new research directions in controlling polaritons.

As one example, the group shows that charge-transfer graphene plasmonic cavities can strongly hybridize with phonon polaritons in proximal 2D materials, such as molybdenum oxide (α-MoO_3) that supports **hyperbolic phonon polaritons** with open, directional iso-frequency contours. In particular, placing graphene plasmonic cavities atop α-MoO_3 induces topological transition in iso-frequency contour from an open hyperbola into a closed oval-shaped contour. This fundamentally modifies the polariton topology, opening new pathways for controlling polariton flow in integrated nanophotonic circuits.

In a final experimental direction, the group explores **strain-engineered plasmonics**. Non-uniform strain gradients in suspended graphene can generate pseudomagnetic fields mimicking Landau quantization without external magnets. In hexagonal suspended WO_x–graphene plasmonic cavities actuated by local back gates, Prof. Kim's team observes suppression of bulk plasmon response with residual edge-localized modes—consistent with Landau level formation. These features suggest the opening of topologically nontrivial plasmonic gaps.

Conclusion: A New Fabrication Paradigm for 2D Polaritons

Prof. Brian Kim's work represents a paradigm shift in the fabrication and control of polaritons in graphene and vdW heterostructures. By using work-function mismatch and self-limited oxidation to create nanometer-precise ambipolar doping patterns, his team has removed the reliance on gates and etching—longstanding obstacles in 2D plasmonics.

The ability to write, tune, and couple high-Q plasmonic cavities directly into pristine graphene opens new frontiers:

- Tunable infrared photonics without lossy gating structures.
- Hybrid polaritons with engineered dispersion in vdW stacks.
- Topologically robust modes via strain and dual-surface doping.

Prof. Kim's research demonstrates that subtle electrostatics, carefully applied, can redefine what is possible in 2D polaritonics—ushering in a new era of precision-engineered nanophotonics and nanoplasmonics.

References

1. Choi, M. S., Nipane, A., Kim, B. S. Y., Ziffer, M. E., Datta, I., Borah, A., Jung, Y., Kim, B., Rhodes, D., Jindal, A., Lamport, Z. A., Lee, M., Zangiabadi, A., Nair, M. N., Taniguchi, T., Watanabe, K., Kymissis, I., Pasupathy, A. N., Lipson, M., Zhu, X., Yoo, W. J., Hone, J. & Teherani, J. T. High carrier mobility in graphene doped using a monolayer of tungsten oxyselenide. Nature Electron. 4, 731 (2021).
2. Kim, B. S. Y., Sternbach, A. J., Choi, M. S., Sun, Z., Ruta, F. L., Shao, Y., McLeod, A. S., Xiong, L., Dong, Y., Chung, T. S., Rajendran, A., Liu, S., Nipane, A., Chae, S. H., Zangiabadi, A., Xu, X., Millis, A. J., Schuck, P. J., Dean, C. R., Hone, J. C. & Basov, D. N. Ambipolar charge-transfer graphene plasmonic cavities. Nature Mater. 22, 838 (2023).
3. Ruta, F. L., Kim, B. S. Y., Sun, Z., Rizzo, D. J., McLeod, A. S., Rajendran, A., Liu, S., Millis, A. J., Hone, J. C. & Basov, D. N. Surface plasmons induce topological transition in graphene/α-MoO3 heterostructures. Nature Commun. 13, 3719 (2022).

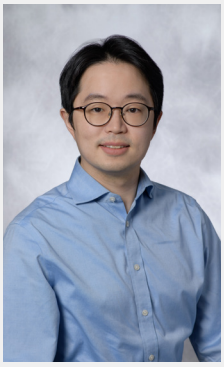

Prof. Brian Kim

About Prof. Brian Kim

Dr. Brian S. Y. Kim is an Assistant Professor of Materials Science & Engineering and Physics at the University of Arizona. He earned his Ph.D. in Electrical Engineering from Stanford University and completed postdoctoral research at Columbia University, specializing in two-dimensional quantum materials and heterostructures. His research focuses on engineering atomically precise quantum systems for advanced electronic, photonic, and quantum technologies, using tools like nano-optical imaging and reconfigurable device architectures. In 2024, he received the Outstanding Young Researcher Award from the Association of Korean Physicists in America and the Korean Physical Society. In 2025, he was named to the Early Career Editorial Advisory Board of APL Photonics and selected as Scialog Fellow in Quantum Matter and Information by Research Corporation for Science Advancement.

NanoScientific Symposium 2025: Global Call for Abstracts

The **2025 NanoScientific Symposium Series** will gather researchers, engineers, and industry leaders at events across Asia, Europe, and the Americas to share the latest breakthroughs in nanoscience and Scanning Probe Microscopy (SPM).

This year's program includes keynote and invited talks from world-renowned scientists, poster sessions, and live demonstrations of cutting-edge instruments. Topics span AFM applications, nanometrology, 2D materials, energy technologies, wafer bonding, correlative microscopy, and beyond. Hands-on sessions and networking events—ranging from academic exchanges to cultural activities—create a truly immersive global forum.

The symposiums will take place from **August through December 2025**, with gatherings hosted in **Korea (Aug 25, Advanced Institute of Convergence Technology), Europe (Sept 17–19, Laboratory of Solid State Physics, Orsay, France), India (Oct 15–16, Indian Institute of Science, Bengaluru), Japan (Oct 24, University of Tokyo),** and **the Americas (Dec 2–3, Stanford University, USA)**. Each regional event builds on the shared mission of advancing nanoscale research while fostering collaboration across borders.

Call for Abstracts

Researchers are invited to submit abstracts for oral or poster presentations. Submissions are welcome from all areas of nanoscience and SPM, including new applications, experimental techniques, and instrument innovations.

Why Participate?

- Present your research to an international community
- Gain recognition through poster and oral sessions
- Engage in hands-on learning with advanced AFM and correlative technologies
- Network with leading scientists and industry experts
- Access recorded presentations and further training through **NS On-Demand and NanoAcademy Online**

For abstract submission guidelines, deadlines, and registration details, please visit the official NanoScientific Symposium website: www.nanoscientific.org .

About NanoScientific Symposium

The **NanoScientific Symposium Series**, sponsored by **Park Systems**, is an international platform dedicated to advancing nanoscale research and applications. By connecting global communities in nanoscience, the symposium promotes knowledge exchange, collaboration, and innovation in next-generation microscopy and metrology.

NanoScientific Highlights Strong Growth in Atomic Force Microscopy (AFM) Market, with Park Systems Recognized as the Global Leader

August 20, 2025

The global nano metrology landscape is entering a new era of growth and innovation, led by the rising demand for atomic force microscopy (AFM) in both research and industrial applications. According to the latest *"Atomic Force Microscopy Market – Global Forecast to 2030"* report by MarketsandMarkets™, the AFM market is expected to grow from **USD 513.6 million in 2024 to USD 762.2 million by 2030**, reflecting a robust **7.1% CAGR**.

This surge underscores the increasing reliance on AFM as a central tool in semiconductor development, advanced materials research, and life sciences—areas where nanoscale precision is indispensable. Nano metrology continues to evolve beyond traditional imaging, expanding into multimodal approaches that integrate AFM with complementary technologies such as digital holographic microscopy (DHM) and imaging spectroscopic ellipsometry (ISE).

Within this expanding market, **Park Systems has been recognized as the number one global AFM company**, holding the highest worldwide revenue share and positioned as a "Star Player" for its combined leadership in revenue and product breadth. The company's proprietary **True Non-Contact™ Mode** and automation capabilities enable high-resolution, non-destructive imaging that is increasingly critical for both industrial quality control and cutting-edge scientific discovery.

The report also notes Park Systems's strategic acquisitions, including Switzerland-based Lyncée Tec SA (DHM), which strengthen its role as a one-stop provider of advanced metrology. This momentum reflects a broader trend: nanoscale measurement is no longer a specialized research tool but a key enabler of progress across industries.

For the nanoscience community, these findings reaffirm that AFM and related nano metrology technologies are not only thriving but also becoming essential drivers of innovation in the decade ahead.

About NanoScientific

NanoScientific is a global platform dedicated to advancing the field of nanotechnology and nano metrology. Through its flagship **NanoScientific Magazine** and a series of **NanoScientific Symposiums held across the Americas, Europe, Southeast Asia, and East Asia**. NanoScientific fosters dialogue among researchers, industry leaders, and innovators. By sharing cutting-edge research, showcasing breakthroughs, and connecting communities worldwide, NanoScientific highlights how nanoscale science and technology are transforming industries and shaping the future. Learn more at www.nanoscientific.org.

Bridging Research and 300 mm Wafer Production

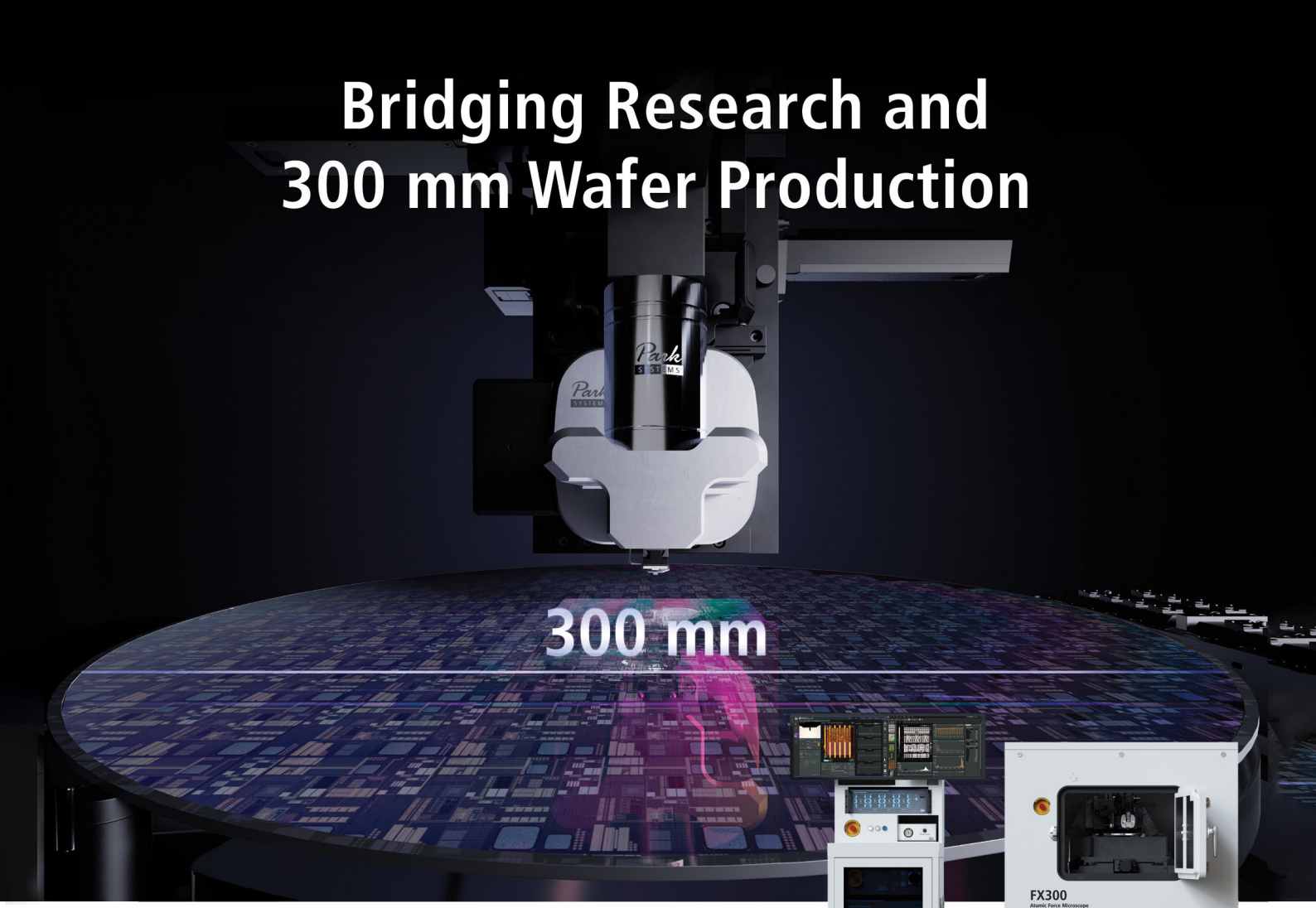

Park FX300

Seamlessly from Lab to Production

Enable smooth transition from lab research to production with the FX300, capable of measuring everything from small samples to full 300 mm wafers. Supporting a wide range of AFM modes, it empowers diverse applications from semiconductor analysis to advanced materials research.

MORE INFORMATION

Engineered for Innovation

Experience automated probe recognition and exchange, instant laser alignment, and SmartScan AI for effortless scaling from R&D to quality control.

Precision You Can Rely On

Achieve sharper, more reliable imaging with lower noise, reduced drift, and a tighter SLD beam, delivering results you can trust.

Park nano-IR Spectroscopy

Combining AFM and Nanoscale IR for Advanced Chemical Characterization

Park nano-IR integrates nanoscale infrared spectroscopy with atomic force microscopy to deliver advanced chemical and materials characterization. By incorporating the latest in infrared spectroscopy—photo-induced force microscopy—into Park's industry-leading AFM platform, this system offers unparalleled performance in nanoscale analysis.

Park SYSTEMS